ANALYSIS OF PERFORMANCE OF ATC RADAR BEACON SYSTEM IN SATIN

REPORT NO. 8421-1

March 1961

CONTRACT FAA/BRD-266

FEDERAL AVIATION AGENCY
BUREAU OF RESEARCH AND DEVELOPMENT

ANALYSIS OF PERFORMANCE OF ATC RADAR BEACON SYSTEM IN SATIN

by

A. Ashley and L. G. Cole

REPORT NO. 8421-1

Contract FAA/BRD-266

March 1960

This report has been prepared by Airborne Instruments Laboratory for the Bureau of Research and Development, Federal Aviation Agency under Contract FAA/BRD-266. The contents of this report reflect the views of the contractor, who is responsible for the facts and for the accuracy of the data presented herein. The contents do not necessarily reflect the official policy of the Bureau of Research and Development or the Federal Aviation Agency.

FEDERAL AVIATION AGENCY
Bureau of Research and Development

AIRBORNE INSTRUMENTS LABORATORY
A DIVISION OF CUTLER-HAMMER, INC.
Deer Park, Long Island, New York

TABLE OF CONTENTS

LIST OF ILLUSTRATIONS

Figure

ABSTRACT

This report presents the results of a study of the use of the Air Traffic Control Radar Beacon in SATIN. A beacon code-usage plan that provides for display filtering in both manual and automatic systems is developed. The performance of the AN/FST-2 as a beacon data processor is analyzed; this includes target detection, release, center marking, and code readout. Deficiencies in code-readout performance are indicated and possible remedies are suggested. The code-processing performance of the AN/FSQ-7 is analyzed; performance is adequate when the AN/FST-2 deficiencies are corrected.

I. INTRODUCTION

The Federal Aviation Agency is investigating the use of SAGE Air Defense System for enroute air-traffic control. The program of SAGE Air Traffic Integration--and the experimental system used in this program is known as SATIN. The Air Traffic Control Radar Beacon System (ATCRBS) can be a valuable addition to the SATIN system since it:

1. Improves tracking reliability,
2. Increases coverage,
3. Provides identity information,
4. Assists track flight-plan correlation,
5. Provides capability of automatic altitude reporting.

The purpose of this work has been to provide engineering services and analysis related to the use of ATCRBS in SATIN. Three primary problem areas have been investigated:

1. Development of a beacon code-usage plan,
2. Analysis of beacon data-processing performance of the AN/FST-2,
3. Analysis of beacon code processing in the AN/FSQ-7.

II. DEVELOPMENT OF A BEACON CODE-USAGE PLAN

A. GENERAL DESCRIPTION

ATCRBS has two primary functions:

1. Improve tracking reliability,
2. Correlate identity with position.

The beacon code-usage plan must optimize the efficacy of these functions. The beacon system can provide for display filtering and the transmission of emergency and/or altitude replies. Display filtering can be accomplished in the manual system only when the code-usage plan is properly designed. Use of the SATIN computer can provide display filtering for any code-usage plan. Display filtering in the SATIN system can be accomplished more easily if a proper code-usage plan is adopted. The existing manual system provides a very limited data link since emergencies are indicated by a single specific code. Proposed future expansion of the system can provide for both indication of a communication failure by use of a specific code and automatic altitude reporting using a separate mode and code configuration.

A comprehensive code plan for ATCRBS is essential to permit optimum use of existing and planned facilities and to provide guide lines for development of future systems. Many equipments and systems will ultimately use beacon data. These systems can be classified according to

1. Use--enroute control, or transition and terminal control;
2. Degree of automaticity--manual or automatic.

The code-usage plan must satisfy all users and permit full exploitation of the capabilities of sophisticated systems without penalizing the users of less sophisticated systems.

The requirements of enroute controllers are similar throughout the United States control area. Thus, a national code-usage plan for enroute control using a portion of the codes should be developed. Terminal-area code usage is a dominant function of each local situation. With the guidance of the Federal Aviation Agency, the regional offices should formulate detailed terminal code-usage plans, using a portion of the codes not used for enroute control.

Automatic computer systems can function with any prescribed code-usage plan. Development of a specific plan simplifies the operation of computer systems while optimizing efficiency. Delay in development of a code-usage plan will cause additional programming delays before efficient use of the beacon codes is attained.

Manual sites have (1) no decoding capability, (2) single-channel decoders, or (3) multichannel (10-channel) decoders. Using single-channel decoders in an area adjacent to an area equipped with multichannel decoders restricts the code usage to a single code at the boundary between the two areas. Single-channel decoders can, however, be easily modified to decode 8 or 16 codes (by disabling three or two delay line taps, respectively) so that increased use of the codes is feasible at the boundaries. Hence, the code-usage plan divides the codes into particular groups of 8 or 16 codes that can be decoded by a modified single-channel decoder. The unused delay-line taps can be selected in several different ways to yield different groupings of the codes. Each grouping would then have a different meaning. For example, if delay-line taps B_1, B_2, and B_4 are disabled, codes 00, 01, 02,..., 07 constitute a group and can be used to designate all aircraft in a particular altitude stratum. If delay-line taps A_1, A_2, and A_4 are disabled, codes 00, 10, 20,..., 70 constitute a group and can be used to designate all climbing aircraft.

Appendix A shows that codes assigned at random should be allocated in proportion to the aircraft density within the respective airspace. This will minimize the probability of redundancy in identity between aircraft on the same code. This is true if the controller can distinguish between aircraft on the same code with the same ability. The result should approximate a random distribution regardless of the method used for assigning codes for enroute traffic. The assignment of codes in the enroute areas should be a function of the density of traffic.

Flow of traffic in the terminal area is more uniform and under stricter control than in the enroute area. Sequential code assignment for approach and departure permits greater separation between aircraft on the same code. The relative separation is always maintained in the terminal area, where traffic densities tend to be higher. The overall effect is that fewer codes are required for the terminal area than for the enroute area.

It is recommended that 32 codes be assigned to the enroute area and 8 or 16 codes to the terminal area. Appendix B shows the probability of false targets and garbled codes as a function of the number of information pulses per reply. The probability of false targets increases with number of information pulses while the probability of garbled codes decreases. Traffic in the terminal area tends to be dense--hence more critical if bracket decoding is used, codes with a minimum number of information bits should be assigned for terminal-area use to minimize the number of false targets. If bracket decoding is not used in the terminal area, codes with many information pulses should be used in order to minimize code garbling. Hence, codes 00 through 17 (with an average of two information pulses) are assigned to the terminal area, whereas codes 20 through 57 (with an average of three

information pulses) are assigned to enroute areas under the assumption that some bracket decoding will be used. Codes 60 through 76 (code 77 for emergency) are reserved for NORAD use and future expansion.

B. ENROUTE PLAN

The enroute airspace is divided into two major horizontal strata on a national basis. For a large portion of the enroute airspace, the lower major stratum is subdivided into two minor strata. An enroute aircraft will usually remain within a particular stratum throughout most of its flight. Climbing or descending near terminals is one notable exception.

The lowest minor altitude stratum is from 0 to 14,500 feet, the intermediate altitude stratum is from 15,000 to 23,500 feet, and the high altitude stratum includes everything above 24,000 feet. Assignment of codes to enroute aircraft as a function of stratum minimizes the number of code changes that the pilot must perform. It also permits filtering of the ground controller's display. A study of dense traffic in the New York Center on 10 July 1959 gives information on distribution of traffic in the various strata in this area. Table I shows the daily density distributions at several typical fixes in the New York Center.

TABLE I

PEAK DAY AIRCRAFT COUNTS IN THREE ALTITUDE STRATA FOR FIVE ENROUTE FIXES, 10 JULY 1959 (PEAK DENSITIES UNDERLINED)

	Altitude Strata		
	Low	Intermediate	High
Allentown	195	62	<u>122</u>
Philipsburg	282	153	95
Harrisburg	340	61	14
Coyle	<u>503</u>	80	12
Wilkes-Barre	456	<u>175</u>	4

A code assignment in proportion to the peak densities shown should use 20 of the 32 enroute codes for low altitudes, 7 for intermediate altitudes, and 5 for high altitudes. Since assignment of codes in groups of 8 or 16 provides an easy method of display filtering, 16 codes should be assigned for low altitudes, 8 for intermediate altitudes, and 8 for high altitudes. This code distribution probably overemphasizes the lower altitudes since the trend in the distribution should be toward higher altitudes and since beacon implementation is more common among the aircraft at higher altitudes. Hence, the code distribution should be modified as follows:

Low altitude and intermediate altitude: 16 codes (codes 20 to 37)

High altitude: 16 codes (codes 40 to 57)

The probability of code redundancy between aircraft on the same code in the enroute area could be reduced marginally by using a sequential assignment of codes at the enroute fix where an aircraft initially reaches its enroute stratum. However, it is desirable to file codes in the flight plan. Therefore, codes should be sequentially assigned for each airway in accordance with filed flight plans. This assigned code could be used by the aircraft throughout its flight profile except for the terminal area and the climb and descend maneuvers through lower or higher altitude strata.

Decoders can be designed to indicate all climbing aircraft by identifying a zero in the second octal code digit (that is, 00, 10, 20, 30, 40, 50). Similarly, a seven in the second digit can be used to indicate a descent.

C. GUIDE LINES FOR TERMINAL-AREA USE

The flow of arrival traffic has an entirely different character from the flow of departure traffic. Handoffs from the Center to the Tower occur at random because

several inbound routes generally feed aircraft to a single "route terminating fix" or feeder fix. Also, the range of aircraft ground speeds makes the prediction of arrival sequence difficult with current methods.

ATCRBS does not appreciably aid the approach controller to identify aircraft actually in a stack because there may be more than 10 aircraft in a 3-by-10-mile area. All aircraft will be flying the same racetrack pattern and code garble probabilities are high. The code assigned by the Center could be used until the aircraft leaves the stack. Change to a Tower code provides positive identification to the approach controller. Thus, substantial assistance is provided when an aircraft leaves the stack.

Single-stack and double-stack operation of a single airport will be examined. The discussion will then be extended to include a complex airport situation. Generally, a radar controller handles only one stack. If no aircraft are holding, the inbound aircraft are sequenced in the order that they are given to approach control. With stacking, the normal sequence is lowest aircraft first, regardless of his speed. As soon as an aircraft leaves the stack to be vectored to the final approach gate, the approach controller can identify him by switching his code or by asking the pilot to IDENT. A number of codes for a stack would be convenient, but two codes are sufficient and even a single code could be used. Using the codes alternately as aircraft are pulled from the stack provides a spacing of at least 6, and normally 8, nautical miles between aircraft with the same code. Slack traffic conditions would permit the use of a single code from the assigned pair.

Radar makes the simultaneous operation of two stacks feasible. Path stretching permits intermeshing of two "trains" of aircraft into a single train at the final approach gate with

minimum longitudinal spacing. If each stack has a pair of codes allotted to it, one airport would use four codes for arrivals. The four codes would not necessarily always be in a repeating sequence at the approach gate, but this is not important for identification.

On the basis of two stacks per airport and two codes per stack, 16 codes are required for four airports in a multi-airport environment. Economies are possible--for example, stacks remote from each other may use the same code pair. Eight codes per terminal area are sufficient. Each terminal area in the country may use the same codes.

Departure traffic is not random. The Center releases each take-off and specifies the departure route, climb procedure, and enroute altitude; hence, fewer codes are required for departure.

The best code distribution for departure appears to be by enroute fix destination, regardless of airport departure. One code for each "route starting fix" at the perimeter of the terminal area is desirable. If there are more fixes than the number of codes allocated to departures, some duplication of codes would not cause serious degradation of system performance.

Codes are also required for terminal-area use where two terminal areas adjoin each other and aircraft proceed directly from one terminal area to another.

D. STEEP-GRADIENT AIRCRAFT

At present, helicopters are not a problem for radar controllers to identify because of their slow speed and small numbers. Shortly, helicopters will be flying that will have 140 knots cruise speed and Instrument Flight Rules (IFR) capability. In the future, Short Take-off and Landing (STOL) and

other types of Vertical Take-off and Landing (VTOL) aircraft will be operating out of sites remote from major airfields, and traffic densities will increase. Some provisions should be made in the code-assignment plan for unconventional operations such as inter-heliport flights. When NORAD releases the codes currently under their control, some of these codes can be allocated to steep-gradient aircraft.

III. ANALYSIS OF BEACON DATA-PROCESSING PERFORMANCE OF AN/FST-2

The AN/FST-2 processes not only radar data but also beacon replies at each beacon site and transforms resulting targets into computer language suitable for transmission over a telephone line to the AN/FSQ-7. Processing includes automatic target detection, determination of range and bearing, label (that is, Pulse X, Mode 2, or Mode 3/A return), and code of the target. Processing is logically reduced to two categories: target detection and location, and code processing.

A. TARGET DETECTION AND LOCATION

The detection criterion used in the AN/FST-2B in the SATIN system assigns a value of +2 for each bracket-decoded reply and a value of -1 for each missed reply. Successive sweeps are examined within a given fixed-range increment or quantum until the algebraic sum of the counts due to hits and misses equals or exceeds 13 (negative counts are not permitted). Similarly, after detection, a value of +2 is assigned to a miss and -1 to a hit. The end of the target is noted when the new algebraic sum equals or exceeds 13 (negative counts are not permitted). The target azimuth (center mark) is chosen at the mid-point between detection and release azimuths.

The AN/FST-2 data processor functions as a defruiter for nonsynchronous replies since the detection process relies upon synchronous behavior. The performance of the AN/FST-2 as a defruiter for target detection has been analyzed previously;*

---

* A. Ashley, et al., "Improved Military Beacon Program," Vol 2, Airborne Instruments Laboratory, Report No. 4569-1, January 1960. (SECRET)

the AN/FST-2B was found to be an effective defruiter for discriminating against false targets generated by fruit replies.

The distribution of detection and release probabilities is a function of (1) the round reliability of each independent interrogation, (2) the detection and release criteria, (3) the interlace ratio, and (4) the mode settings on the transponder. Round reliability is a figure used to indicate the ratio of the number of valid replies available to the number of valid interrogations. There are three Mode 3/A interrograations and one Mode 2 interrogation in the SATIN system interrogation cycle. Civil aircraft can reply only to Mode 3/A interrogations, whereas military aircraft can reply to both. Military aircraft are assumed to reply to all interrogations in this report.

Probabilities of detection and release as a function of the number of hits per beamwidth were computed as described in Appendix C. Round reliability remains constant for military aircraft throughout the beamwidth. Round reliability equals zero for civil aircraft on every fourth interrogation because of the mode interlace. The probabilities were computed for civil aircraft for each of four possible starting points in the interlace cycle. The cumulative probability of detecting a military aircraft as a function of round reliability and number of hits per beamwidth is shown in Figure 1. Figure 2 shows the probability of release as a function of hits after detection. Figures 3 and 4 depict the probabilities of detection and release, respectively, for a civil aircraft. It is concluded that civil aircraft are harder to detect and easier to release.

The results of the detection and release analyses were combined to determine the probable position of the center mark. Although the AN/FST-2B determines the target center in units of azimuth pulses (4096 azimuth pulses equals 360 degrees),

this analysis was done in terms of hits (4680 hits equals 360 degrees) to simplify calculations. An antenna with 50 hits per beamwidth was assumed. The probability of center marking at N hits after start of the beam was determined by multiplying the probability of detection at N - n hits by the probability of release at N + n hits and summing for all possible values of n. This process is straightforward for the military case since the probabilities are independent of the position of the interlace cycle on the first trial or hit. It was necessary to consider the position of the interlace cycle for the civil case and to determine the probability for each possible initial position of the cycle; the resultant probability is the average of all four position probabilities since each position is equally likely. N assumes integer and half-integer values. The AN/FST-2 center marking corresponds more closely to integer values of N only. Hence, the probability densities at the integer value and the next higher half-integer value were summed to obtain the resultant density function.

Figure 5 shows the distribution of the center mark. The distribution of the center mark was successfully tested against a normal distribution within an 80-percent confidence level (Kolmogorov-Smirnov* tests) in all cases. The average value of the position of the center mark and the standard deviation were determined for each value of round reliability. These values are plotted in Figure 6. The average value is displaced from the beam center in all cases. A correction has been made in the SATIN system in collimating the sites. Since the basis for this correction is different (error between radar

---

* Frank J. Massey, Jr., "The Kolmogorov-Smirnov Test for Goodness of Fit," Journal of the American Statistical Association, Vol 46, No. 253, March 1951.

and ATCRBS), the correction indicated here cannot be compared with that actually used.

B. CODE PROCESSING

The code content of the replies within the beamwidth is examined after detection. Unless a code with a higher priority is received, the first code with the highest priority is stored until the end of the beam. This code and its associated label are available for transmission at the end of the beam. The highest-priority replies have the center pulse (Pulse X) present. Any reply during the beamwidth can be garbled to appear as a special reply if a fruit pulse coincides with an empty center slot. The probability of changing a label to Pulse X has been previously analyzed.* As a result of that analysis, a modification is being developed that requires two Pulse X returns on successive hits; each return must check parity.

Civil aircraft do not reply to Mode 2 interrogations. If a fruit reply that checks parity is received during the time that a reply to a Mode 2 interrogation could be expected, the label will be changed to Mode 2; the code content of the fruit reply is stored. If a code from the desired mode is stored, this code can be garbled. If P_X is the probability of mislabeling as a Pulse X, P_2 is the probability of mislabeling as a Mode 2 return, and P_G is the probability of garbling the code in the desired mode, the probability of getting a correct return on a single scan for a civil target is

$$P = (1 - P_G)(1 - P_X U P_2).$$

---

* See footnote on page 3-1.

For a military target, the probability of getting a correct return on a single scan is

$$P = (1 - P_G)(1 - P_x).$$

These probabilities were evaluated for various fruit rates and a number of post-detection interrogations for the following conditions:

1. Existing AN/FST-2B,
2. The planned modification to require two consecutive Pulse X replies that check parity,
3. A defruiter inserted in the code-readout section of the AN/FST-2B,
4. The planned Pulse X integration modification as in case 2, with an additional modification to require parity check returns (the returns need not be identical) on two successive Mode 2 interrogations,
5. Use of a defruiter as in case 3, but requiring a parity check on Pulse X returns.

The resulting probabilities of a correct Mode 3/A return from a civil aircraft in cases 1, 2, and 3 are shown in Figure 7. Two scales of fruit rate are shown. The fruit rate per second is of particular interest since the probabilities shown are applicable to a target in a heavy fruit sector when the total fruit in a complete scan is low. Figure 7 also shows that wide beamwidth antennas increase mislabeling probabilities and hence decrease the probability of a correct Mode 3/A return. The probability of changing the label to a Mode 2 label is based on the assumption that 60 percent of the fruit will check parity since 50 percent of the Mode 3/A fruit and almost 100 percent of the Mode 2 fruit will check parity. Sixty percent of the total fruit appears to be a reasonable compromise. Figure 8 shows the probability of

a correct Mode 3/A return from a civil aircraft for cases 1 through 5, with 35 hits after detection. All probabilities are based on a round reliability of 0.9. Decreasing round reliabilities reduces the probability of a false label slightly and improves the probability of a correct Mode 3/A code by a small amount.

IV. ANALYSIS OF BEACON CODE PROCESSING IN AN/FSQ-7

Selective Identification Feature (SIF) codes are established for each track in the AN/FSQ-7 when the positional data associated with the code are used for smoothing the track position in three or more consecutive frames. The SIF code becomes disestablished when the code of the data used for smoothing in three consecutive frames is not the established code.

SIF score implements establishment and disestablishment of SIF codes. Scores are kept for Mode 2 and Mode 3/A on each track in accordance with the flow chart shown in Figure 9. Analysis of the performance of the scoring system requires differentiation between establishment in the correct code (code the aircraft is transmitting) and establishment in a code that is garbled in the same way on successive frames. Figure 10 is a modified flow chart, equivalent to Figure 9, that differentiates between true and false codes.

The scoring method was analyzed for each of two sets of initial conditions. The first condition is for a code that has been filed in the flight plan and enters state E3 as soon as the track is initiated. The other condition is for an unfiled code; the flow chart is entered at the ZO state.

The analysis indicates that the probability of an established code is the same for both initial conditions after a sufficient number of scans. Thirty scans were sufficient in all cases, and the difference after 20 scans was negligible in most cases. Figure 11 shows the probability of a code class track (established code) when a single AN/FST-2 provides coverage. Comparison of Figure 11 with Figure 8 for the same

conditions shows that the probability of a code class track is higher than the probability of a correct Mode 3/A code from the AN/FST-2 when the probability of a correct Mode 3/A is greater than about 0.5. Numerical evaluation also shows that the probability of establishment in the wrong code never exceeds 0.0005 even with a pessimistic assumption for probability of a repeated garble.

When a second AN/FST-2 also provides coverage, the probability of at least one correct code during a single frame is increased. Performance of the SIF score with data from two AN/FST-2's was analyzed. Figure 12 shows the results of this analysis and indicates the degree of additional improvement gained by use of dual coverage. Some additional improvements could be expected with more redundant coverage.

Figure 13 shows the performance of the SIF score criterion as a function of number of scans for a fruit rate of 90,000 replies per scan or 6920 replies per second for three different system configurations. The curves indicate that the probability of a code class track is the same after 10 to 25 scans, independent of whether a code was filed. The situation whereby a pilot switches codes automatically without notifying the ground controller was analyzed for the same fruit rate (90,000 replies per scan). The results are shown in Figure 14. Figures 13 and 14 indicate that the probability of establishment of the code increases more rapidly and reaches a higher value when adequate processing (such as integration, parity, and defruiting) are provided.

V. CONCLUSIONS

1. The adoption of a beacon code-usage plan, such as that proposed herein, is necessary to provide optimum use of the beacon system.

2. Beacon codes should be allocated in proportion to the traffic density.

3. The angle-tracking accuracy of the AN/FST-2 is degraded by reduction in beacon round reliability. At low round reliabilities, the positional accuracy is limited at long ranges by angle accuracy rather than by range accuracy.

4. The angle-tracking accuracy of the AN/FST-2 is degraded when the target is a civil aircraft instead of a military aircraft, because of the mode interlace.

5. The average or expected angular position of a target is a function of round reliability and mode sensitivity of the target transponder.

6. The AN/FST-2 is an effective defruiter for target detection.

7. The probability of transmitting a correct Mode 3/A code from the AN/FST-2 on a civil aircraft is not acceptable at high fruit rates. It can be made acceptable by additional integration on code replies or by a revision of the priority system.

8. Mode 3/A codes will not be available in the AN/FSQ-7 from military aircraft unless the priority system or mode interlace cycle is modified.

9. If the additional integration is provided in the AN/FST-2, the SIF score criterion is adequate.

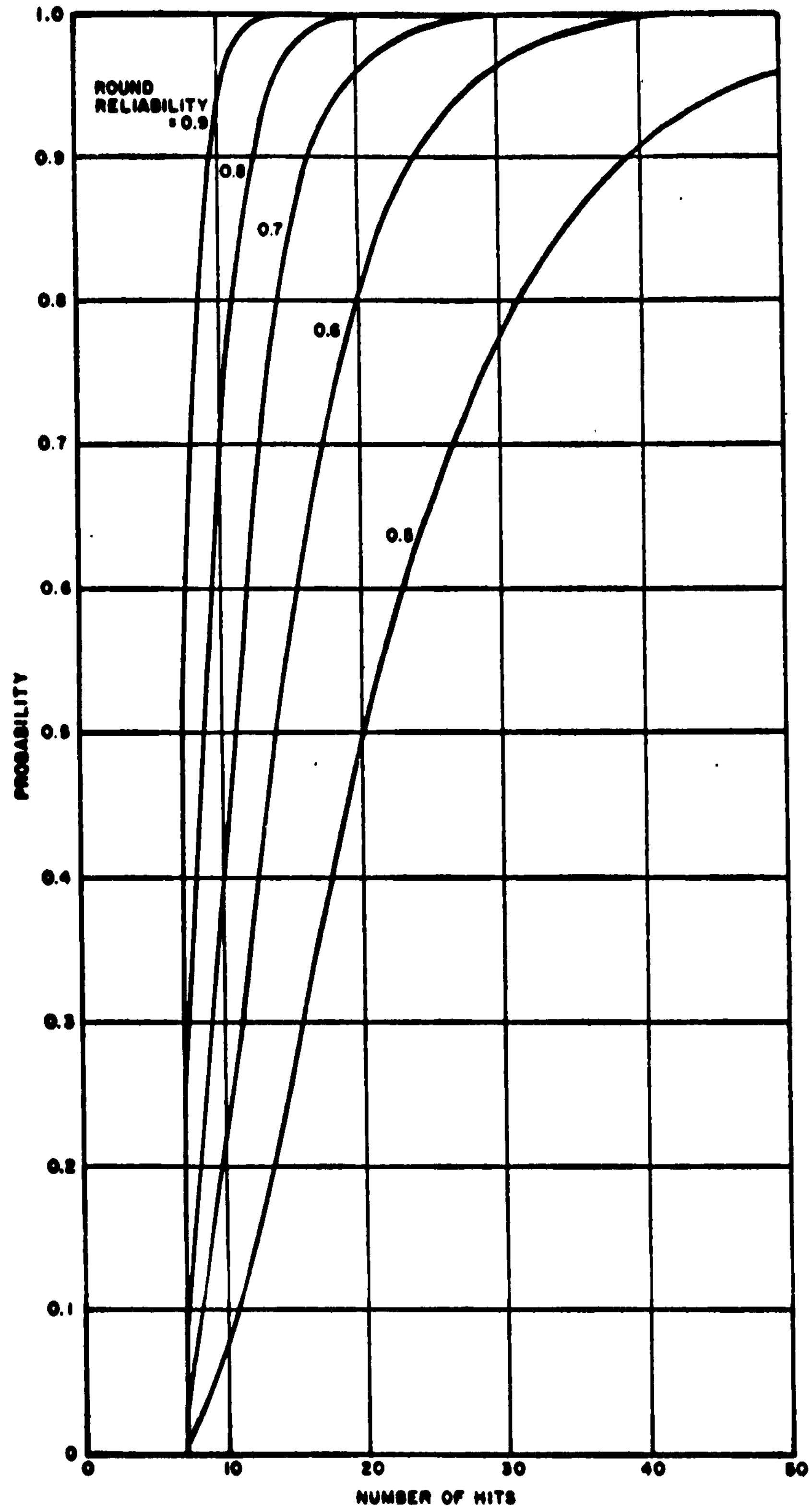

FIGURE 1. PROBABILITY OF DETECTION OF A MILITARY AIRCRAFT AS A FUNCTION OF HITS PER BEAMWIDTH AND ROUND RELIABILITY

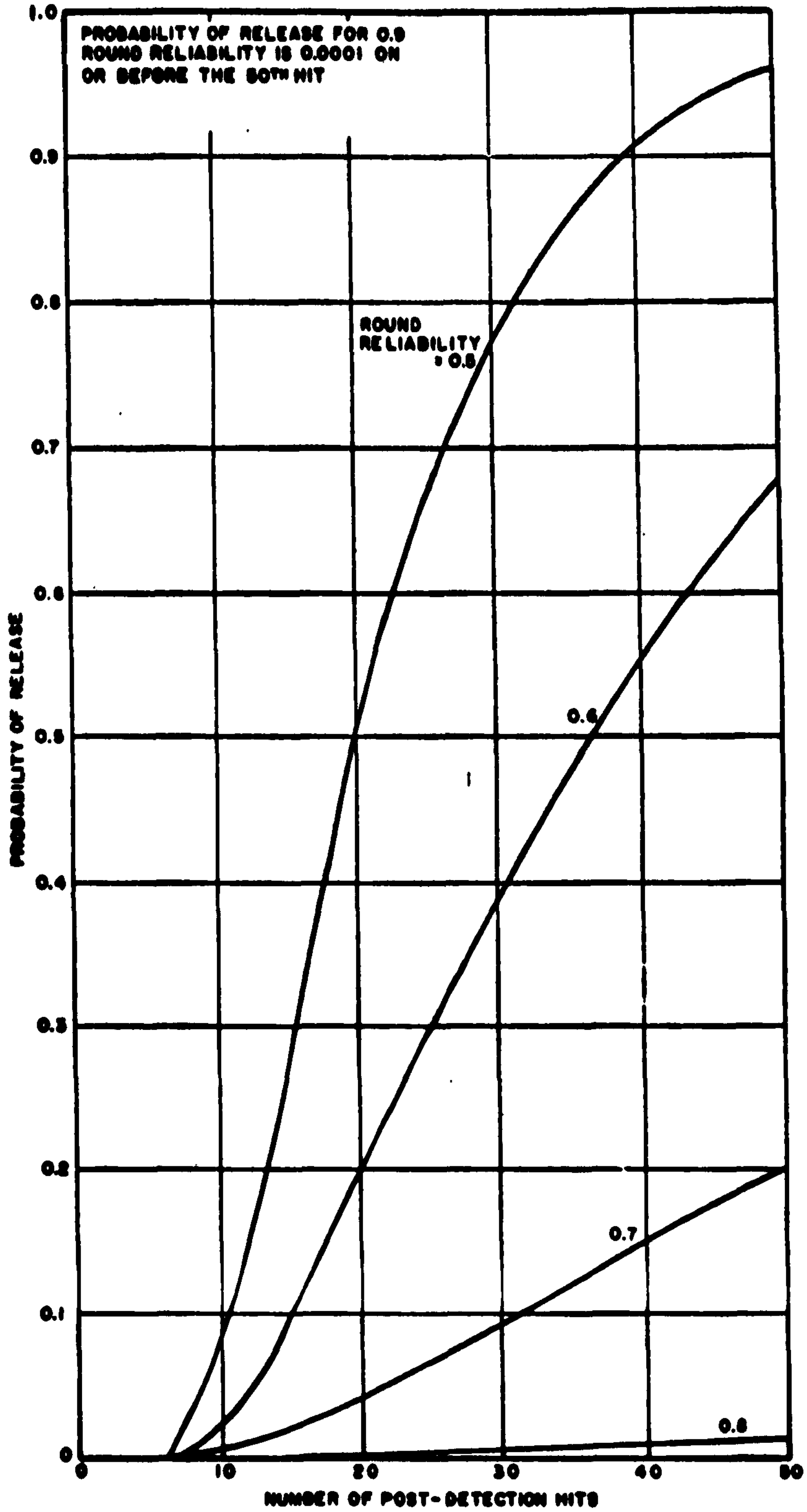

FIGURE 2. PROBABILITY OF RELEASE OF A MILITARY AIRCRAFT AS A FUNCTION OF THE NUMBER OF POST-DETECTION HITS AND ROUND RELIABILITY

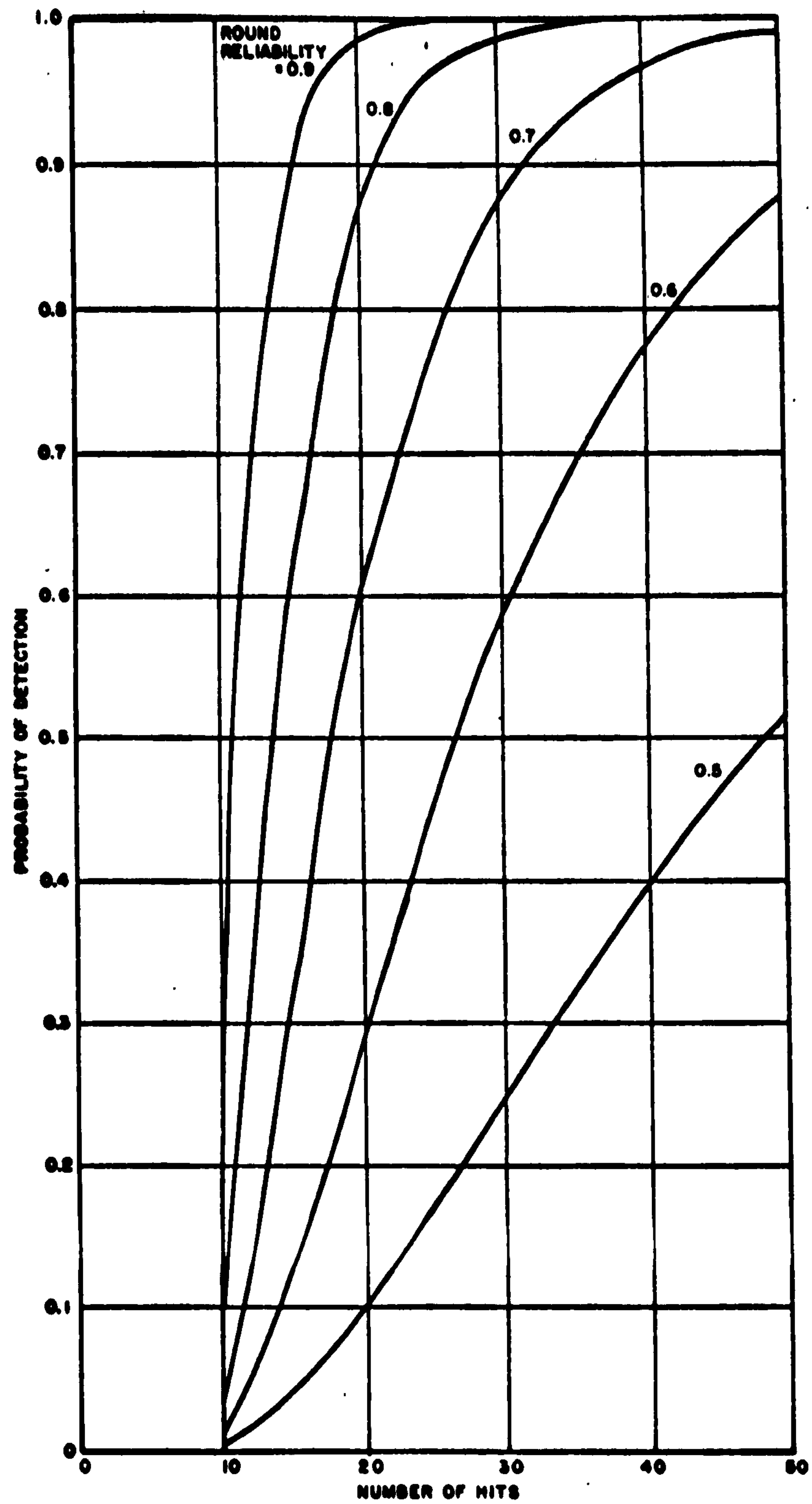

FIGURE 3. PROBABILITY OF DETECTION OF A CIVIL AIRCRAFT AS A FUNCTION OF HITS PER BEAMWIDTH AND ROUND RELIABILITY

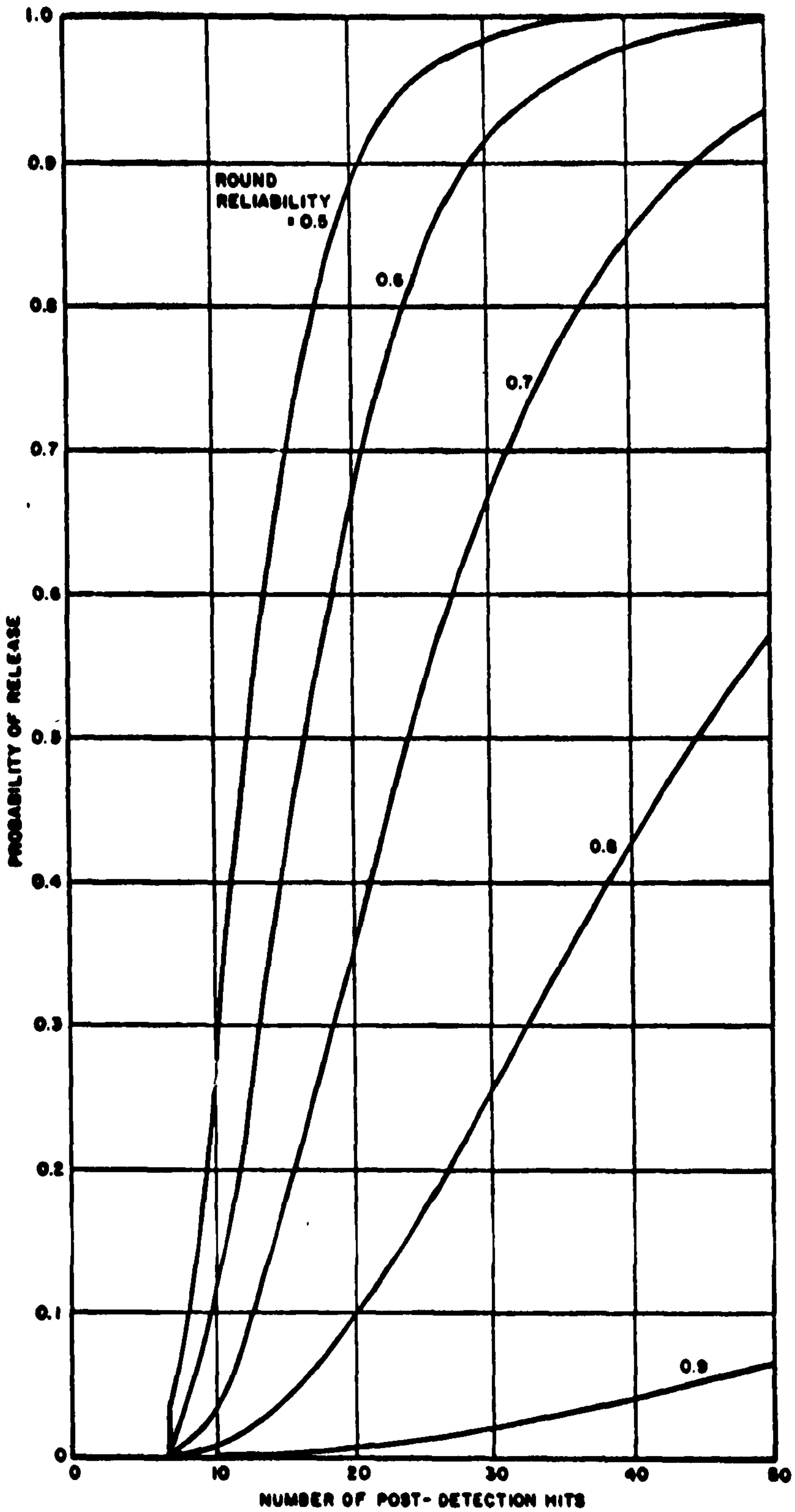

FIGURE 4. PROBABILITY OF RELEASE OF A CIVIL AIRCRAFT AS A FUNCTION OF THE NUMBER OF POST-DETECTION HITS AND ROUND RELIABILITY

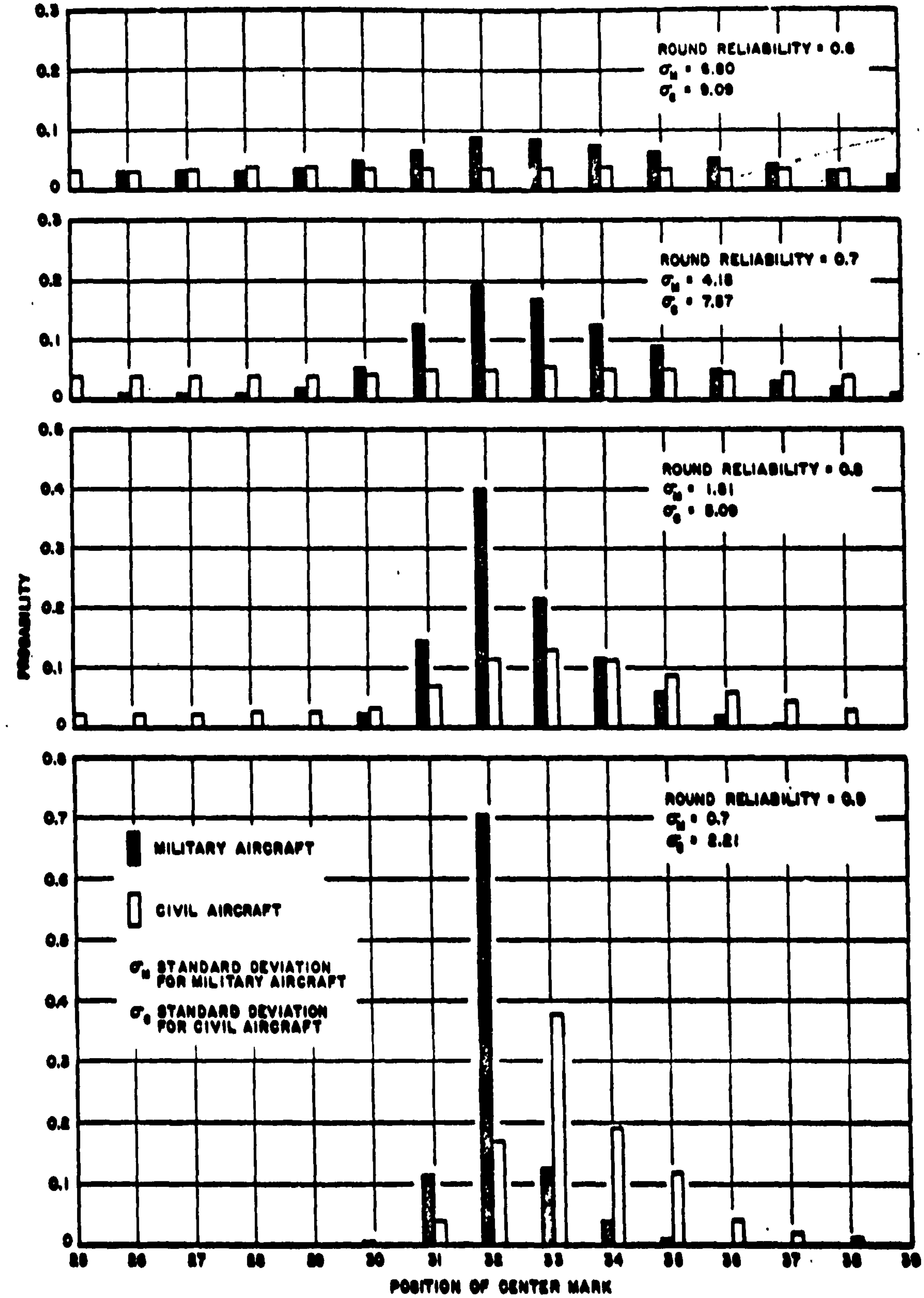

FIGURE 5. POSITION OF CENTER MARK AS A FUNCTION OF ROUND RELIABILITY

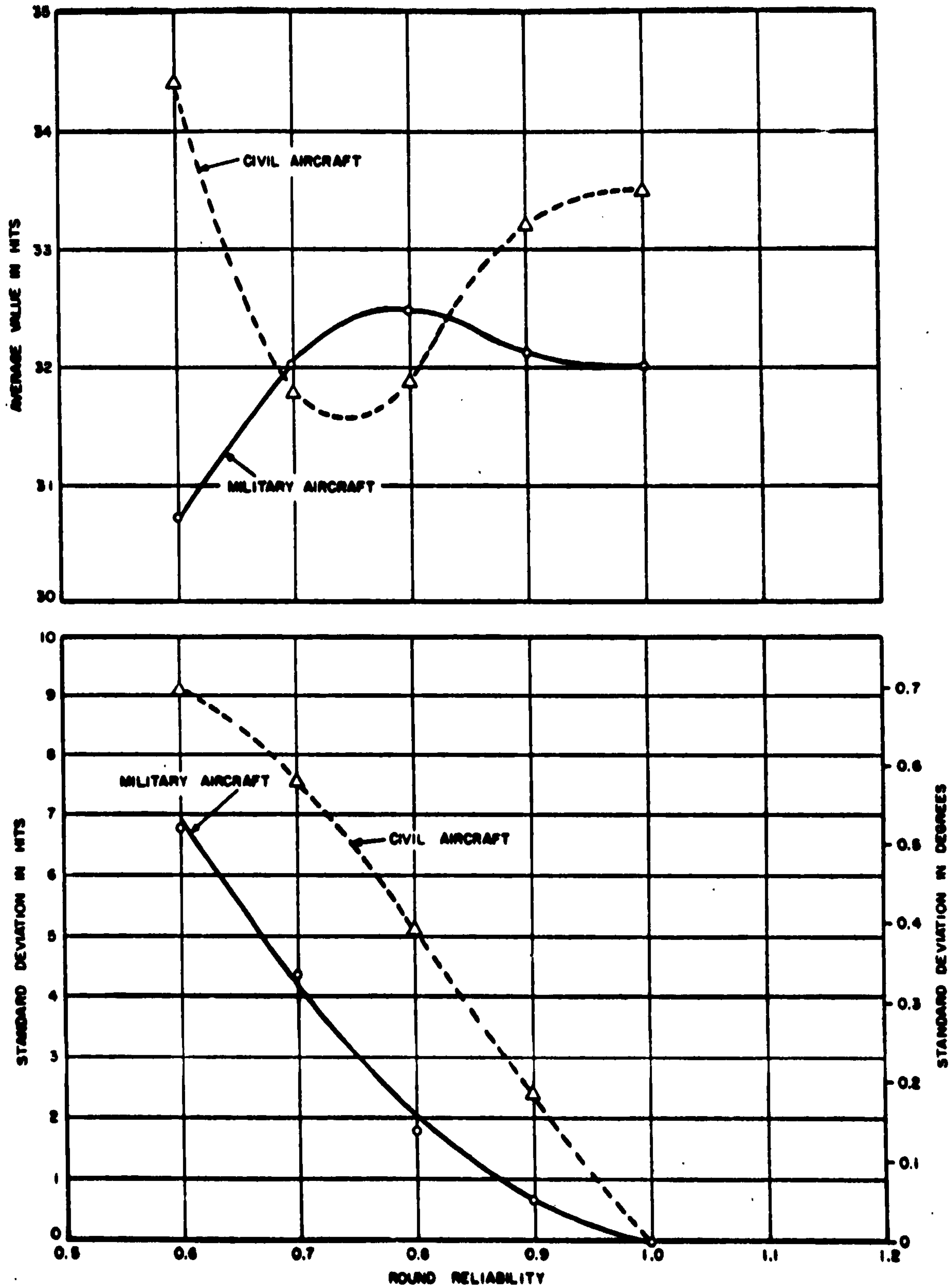

FIGURE 6. AN/FST-2 ANGLE TRACKING ACCURACY WITH A 50-HIT ANTENNA

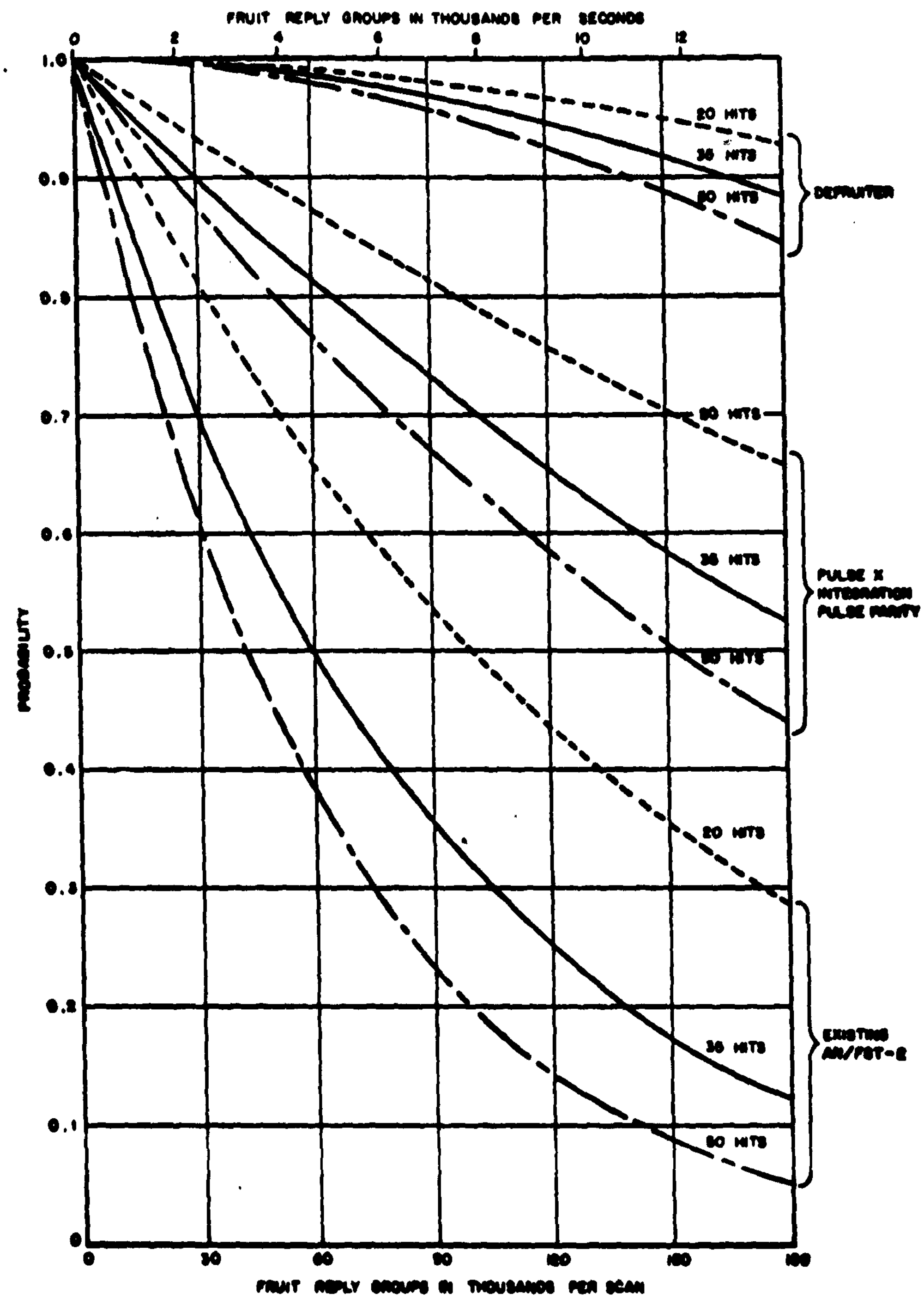

FIGURE 7. PROBABILITY OF CORRECT MODE 3/A RETURN FROM A CIVIL AIRCRAFT WITH 0.9 ROUND RELIABILITY

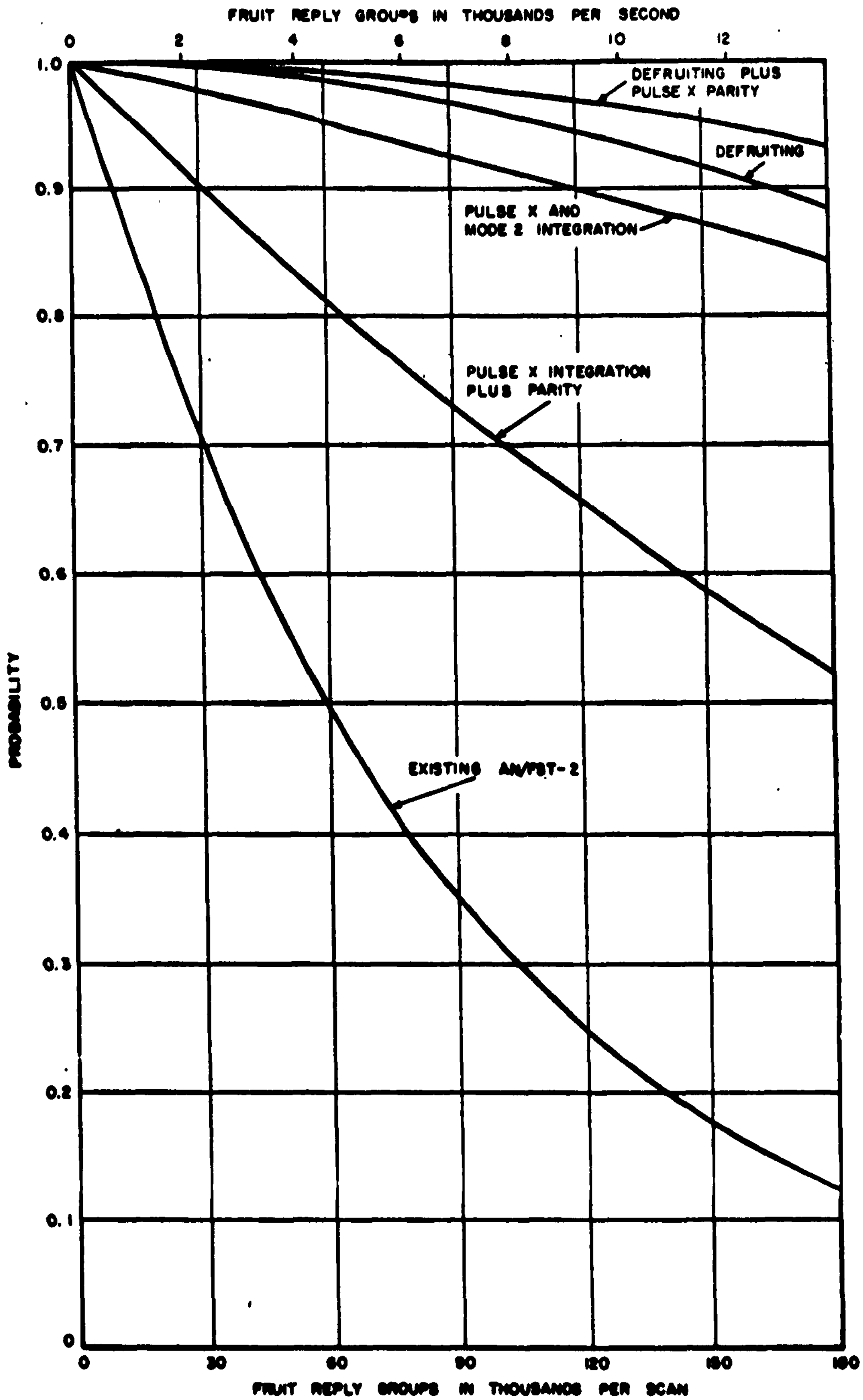

FIGURE 8. PROBABILITY OF CORRECT MODE 3/A RETURN FROM A CIVIL AIRCRAFT WITH 0.9 ROUND RELIABILITY AND 35 HITS AFTER DETECTION

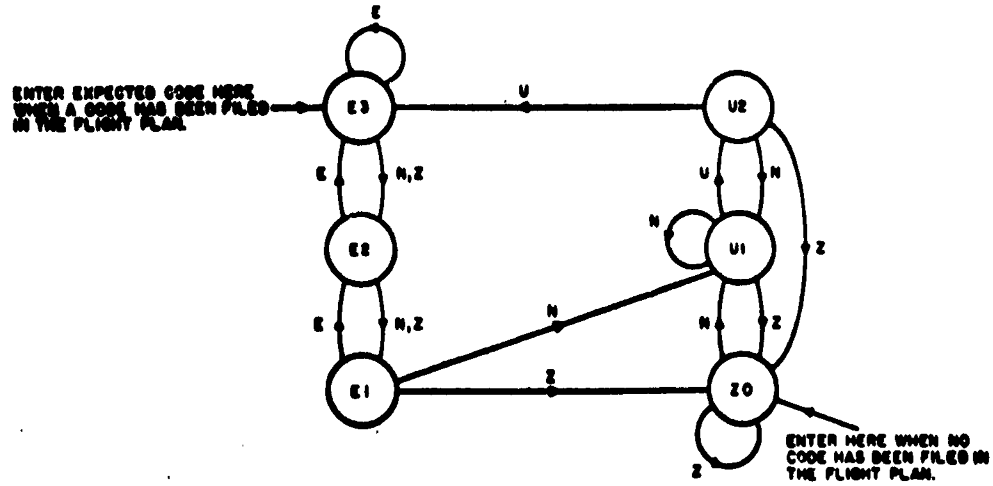

IN CIRCLES

E = A code is established.

U = No code is established but an unestablished code has been stored from the previous frame.

Z = No code has been stored or established.

0, 1, 2, 3 = SIF score for the mode.

ON ARROWS

E = Established code was used.

U = Unestablished code stored last frame was used this frame.

N = New code was used this frame.

Z = No code was stored this frame.

FIGURE 9. FLOW CHART FOR SIF SCORE

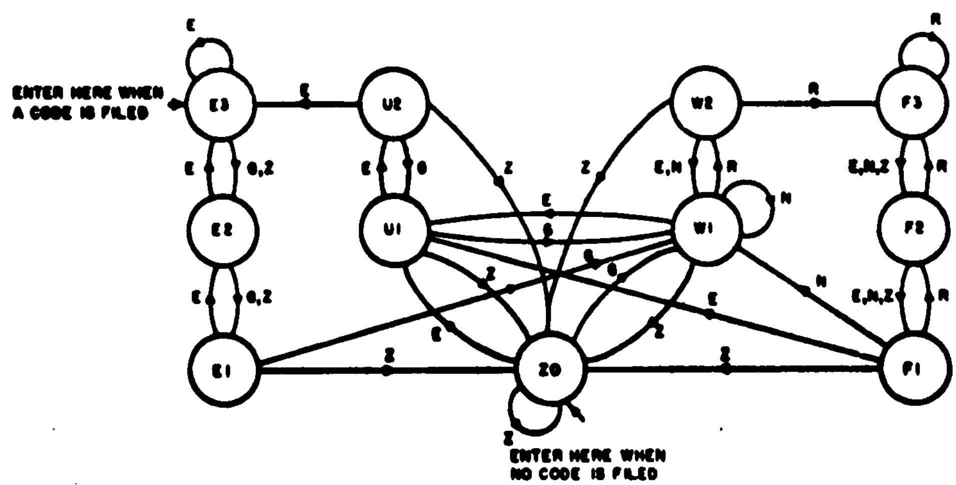

IN CIRCLES

E = A correct code is established.

U = No code is established but a correct unestablished code has been stored from the previous frame.

Z = No code has been stored or established.

F = A wrong code is established.

W = No code is established but a wrong unestablished code has been stored from the previous frame.

0, 1, 2, 3 = SIF score for the mode.

ON ARROWS

E = Correct code was used.

Z = No code was stored.

G = Garbled code was used.

R = Repeated garbled code was used.

N = Nonrepeated garbled code was used.

FIGURE 10. ANALYTICAL REPRESENTATION OF FLOW CHART FOR SIF SCORE

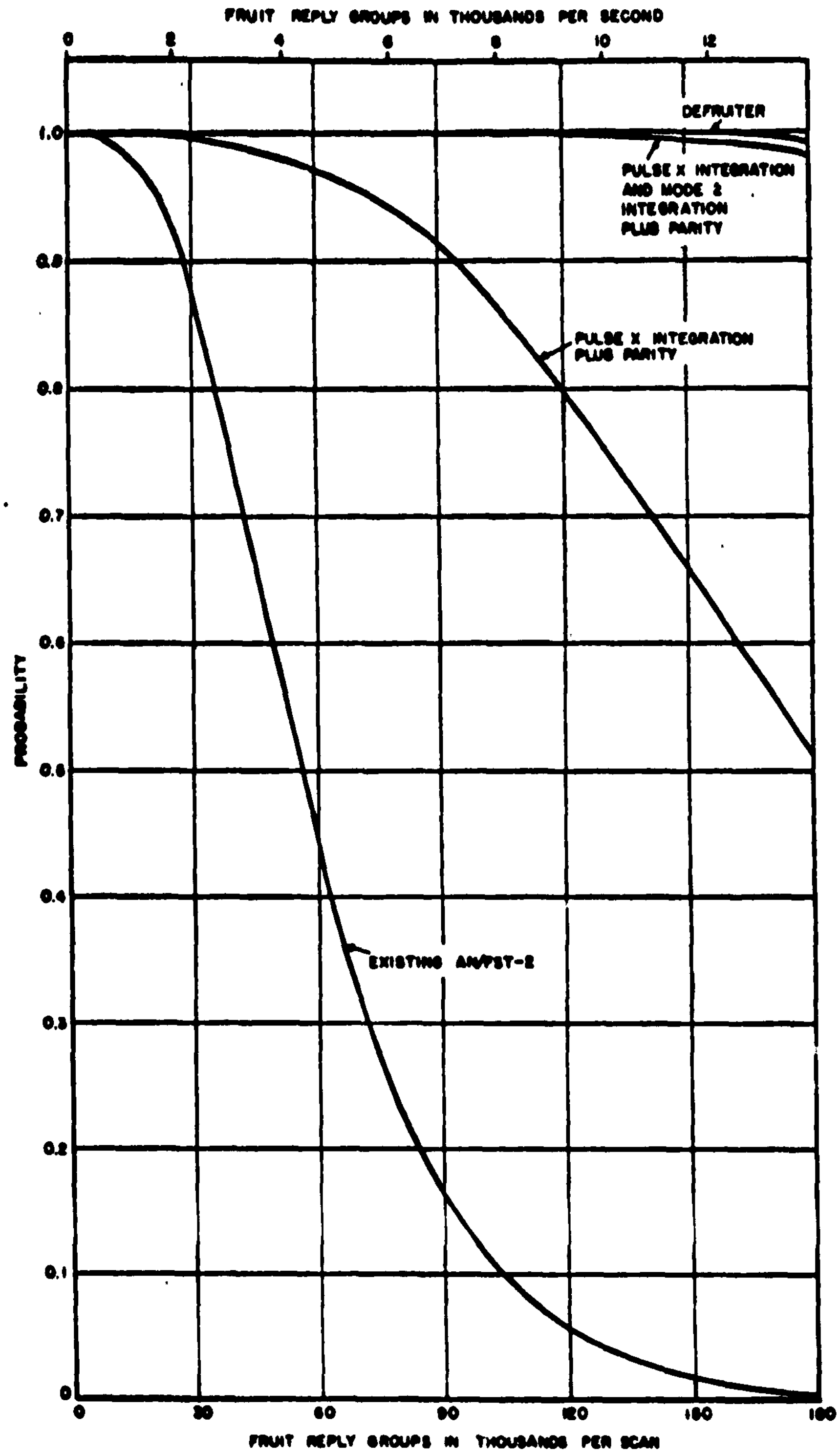

FIGURE 11. PROBABILITY OF CODE CLASS TRACK AFTER 30 OR MORE SCANS WITH SINGLE COVERAGE

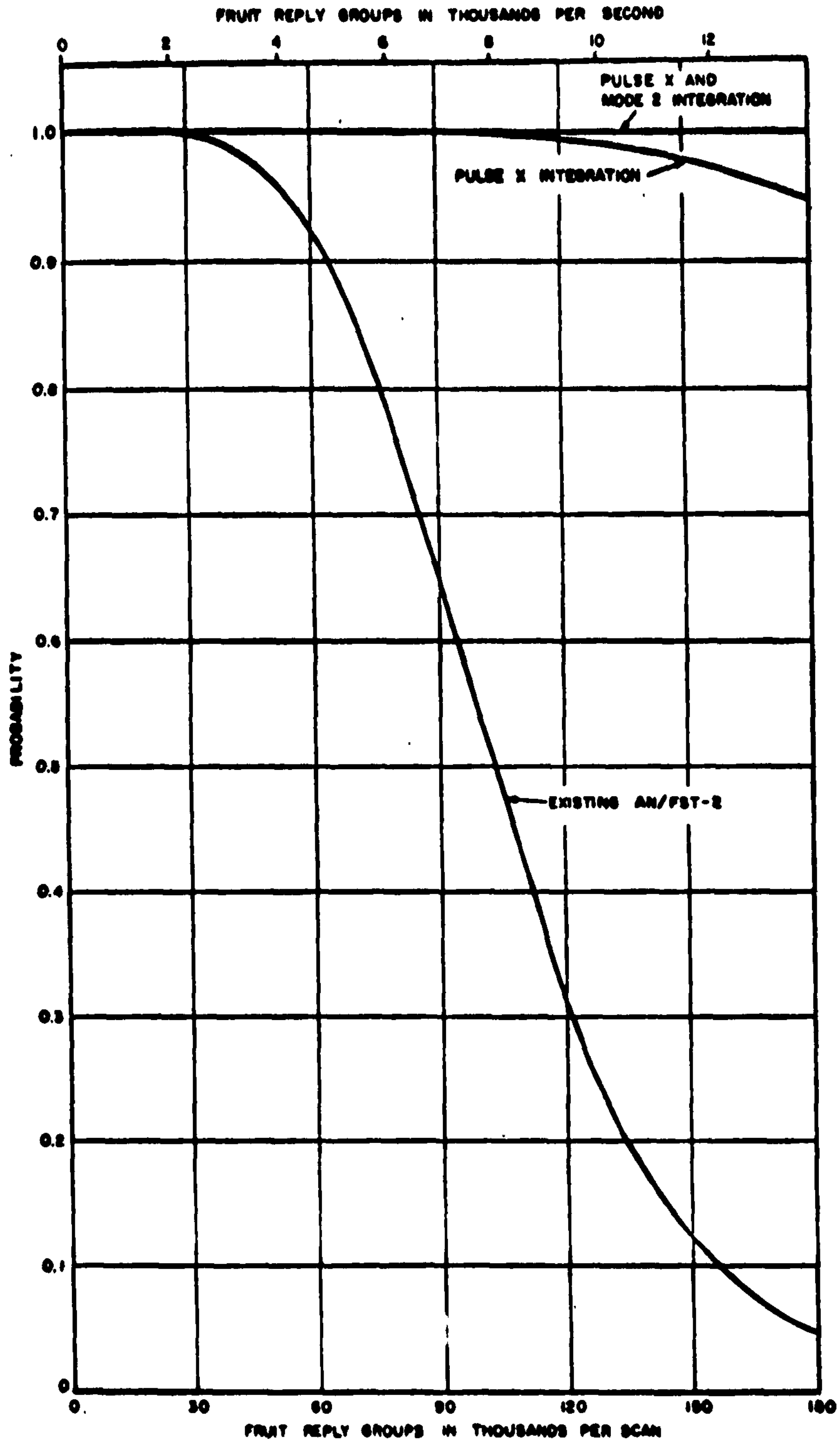

FIGURE 12. PROBABILITY OF CODE CLASS TRACK WITH DUAL COVERAGE

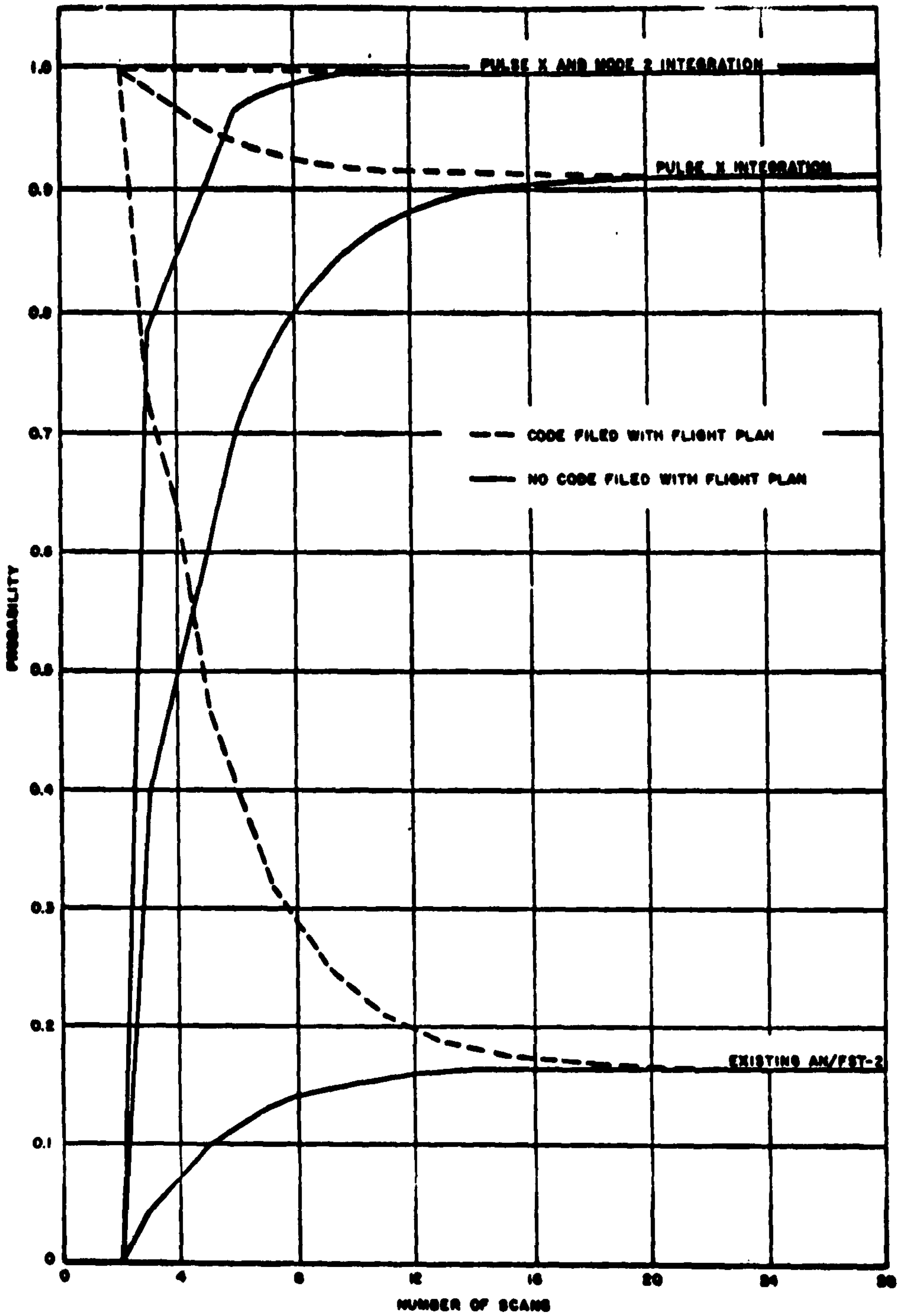

FIGURE 13. PROBABILITY OF CODE CLASS TRACK AS A FUNCTION OF TIME AND INITIAL CONDITIONS FOR 90,000 FRUIT REPLY GROUPS PER SCAN

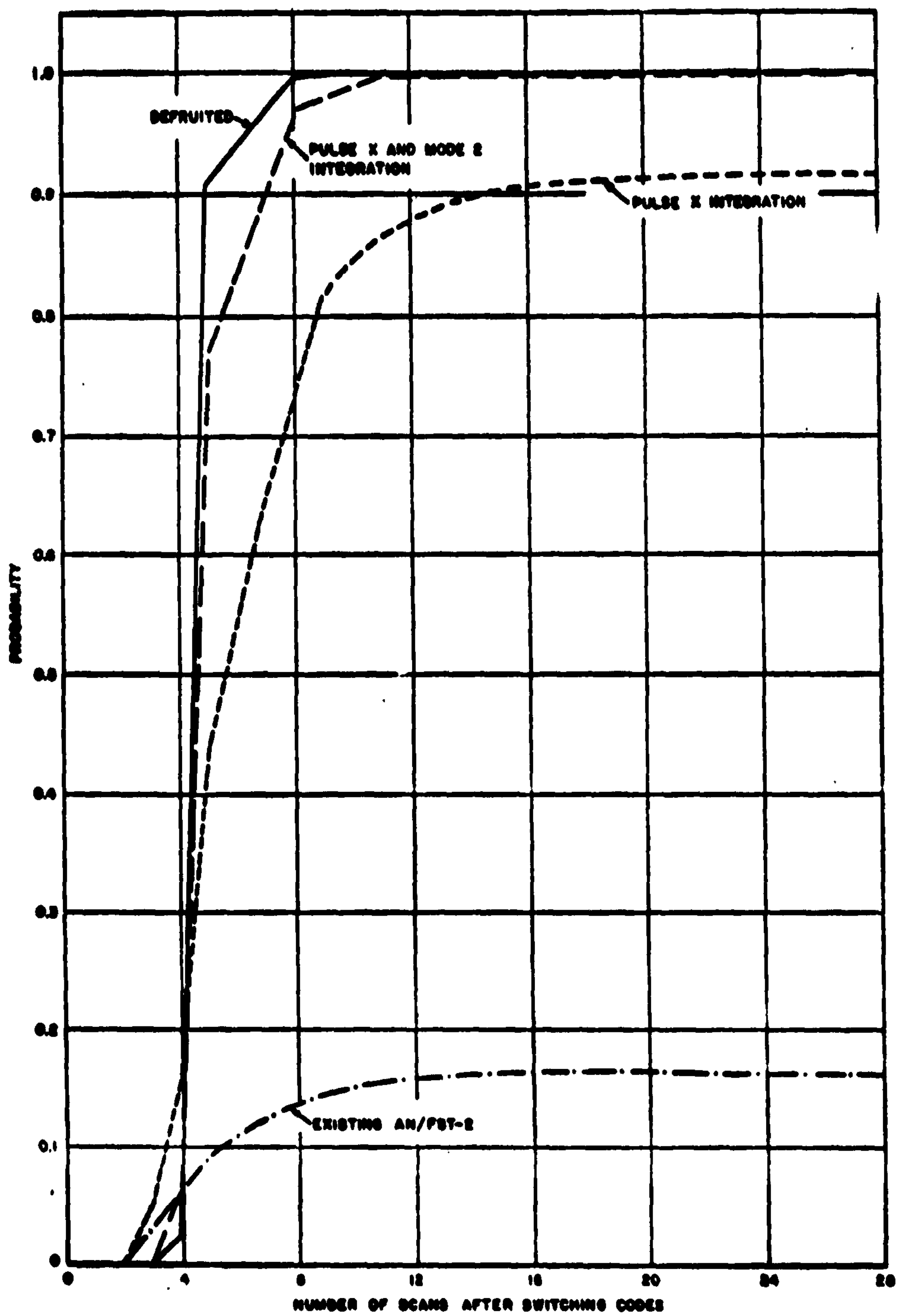

FIGURE 14. PROBABILITY OF CODE CLASS TRACK WITH AUTOMATIC CODE SWITCH FOR 90,000 FRUIT REPLY GROUPS PER SCAN

APPENDIX A
ANALYSIS OF BEACON CODE USAGE

An analytic simulation of air-traffic flow has been developed to provide a tool for evaluating some aspects of the relative performance of various beacon code-usage configurations. Other evaluation techniques will be investigated during the current study. Evaluation is based on predicting the redundancy that results from aircraft using the same code within a prescribed time or distance separation. The parameters of the analytic model are: aircraft density per hour, time or distance separation, and the number of codes assigned to the volume of space under investigation.

A mathematical model technique has been chosen as the most economical method of appraising the relative merits of various code-usage plans since it provides a guide to the simulated test programs, thereby reducing the testing time and costs.

Realism has been maintained by comparing aircraft density data extracted from actual observed data* with results predicted by the theoretical model. The particular data used was taken at the COYLE fix at the intersection of V1 and V16. This fix is the highest aircraft density fix in the New York area; although not within the SATIN area, it represents a typical high-density situation. It will be shown that the

* O. M. Patton and G. E. Cothren, "Data Displays for Operations Analysis of Air Traffic Demands and Delays in the New York ARTCC Area on January 28 and February 28, 1958," The Franklin Institute, Contract No. AMB-3, November 1958.

For two additional aircraft,

$$p(2) = \int_0^T \int_0^{T-t_1} \lambda e^{-\lambda t_1} \lambda e^{-\lambda t_2} e^{-\lambda(T-t_1-t_2)} dt_2 dt_1$$

where t_2 is measured from t_1. Thus,

$$p(2) = \frac{(\lambda T)^2}{2!} e^{-\lambda T}$$

This is the Poisson probability for exactly two events within T. Furthermore, this is the total probability for the three equally probable ways that two additional aircraft can arrive within T of the observed aircraft--two before, two after, and one on each side.

In general, for r additional aircraft,

$$p(r) = \lambda^r e^{-\lambda T} \int_0^T \int_0^{T-t_1} \int_0^{T-t_2} \cdots \int_0^{T-t_{r-1}} dt_r \cdots dt_3 dt_2 dt_1$$

$$p(r) = \frac{(\lambda T)^r}{r!} e^{-\lambda T}$$

or simply the Poisson distribution that exactly r aircraft arrive within T. In each case, the arrival times are each measured from the respective preceding arrival time.

Table A-I compares data taken for five hours of 13-aircraft-per-hour density and predicted aircraft flow using the Poisson distribution.

The results are remarkably good and clearly indicate the applicability of the negative-exponential time distribution.

$$= e^{-\lambda T} e^{\frac{\lambda T(n-1)}{n}}$$

$$= e^{\frac{-\lambda T}{n}}$$

This result is interesting since it proves that the probability of no redundancy for a given aircraft is simply equal to the Poisson probability of zero events within T for an aircraft density reduced by the number of available codes n. The effect of reducing λ by n is to examine only the average number of aircraft on a particular code as an isolated population. Results are plotted for 5, 10, 20, and 40 codes for aircraft densities of 12, 18, 24, and 30 aircraft per hour in Figures A-2 through A-5. A universal curve for $0.1 \leq \lambda \leq 10$ is given in Figure A-6.

If one aircraft is to be observed in each of N volumes of space having a designated number of codes n, the probability that none of the N aircraft will be involved in a redundancy is

$$\prod_{j=1}^{N} \left(e^{\frac{-\lambda_j T}{n_j}} \right)$$

Since this is a product of terms bounded by 0 and 1, the joint probability must be less than or equal to the smallest factor. Hence, the probability is a maximum if all factors are equal. This is achieved by setting λ_j/n_j equal to a constant for all j. In other words, codes should be assigned in direct proportion to average aircraft flow per volume of space.

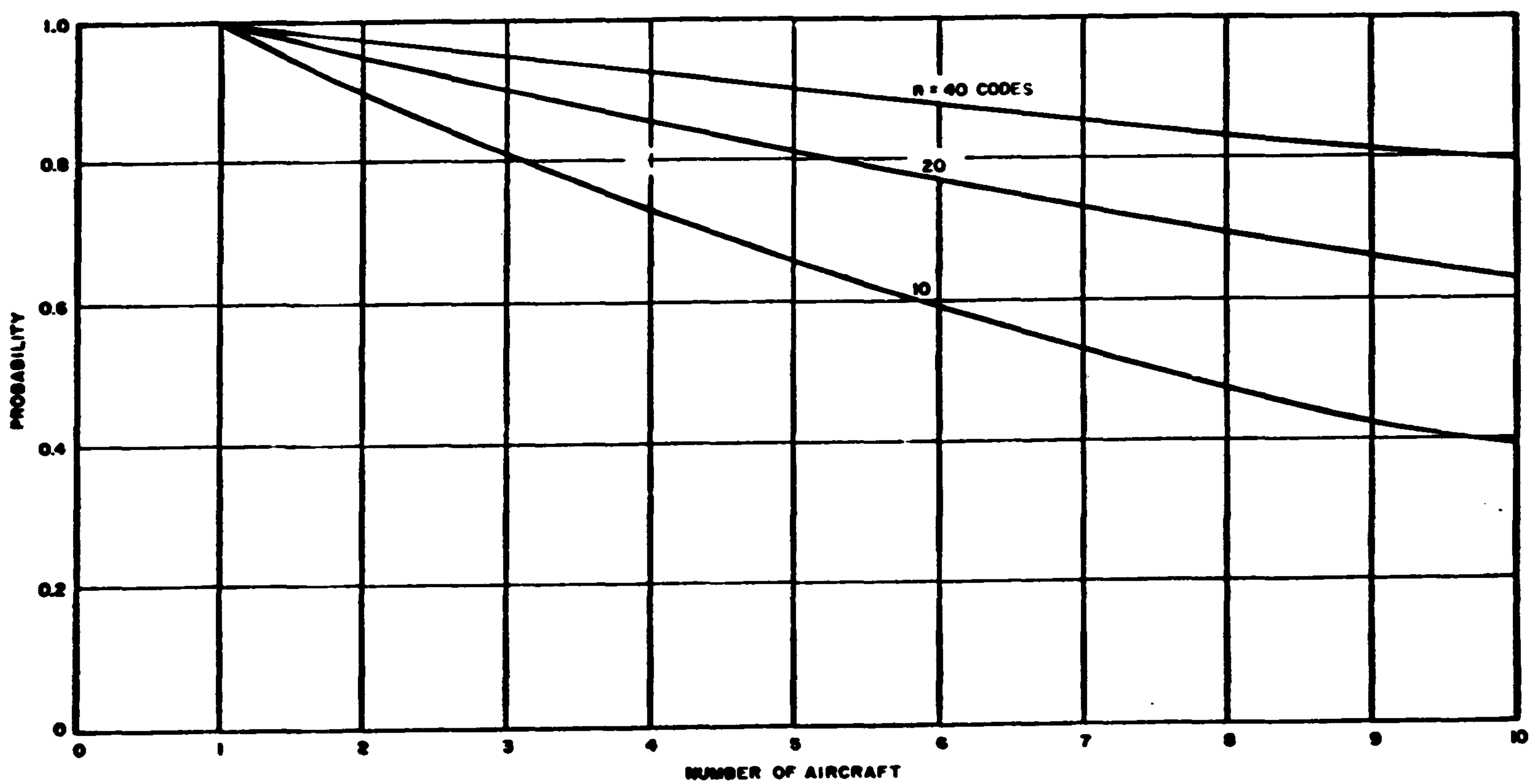

FIGURE A-1. PROBABILITY OF NO CODE CONFLICT FOR AIRCRAFT IN TIME CONFLICT

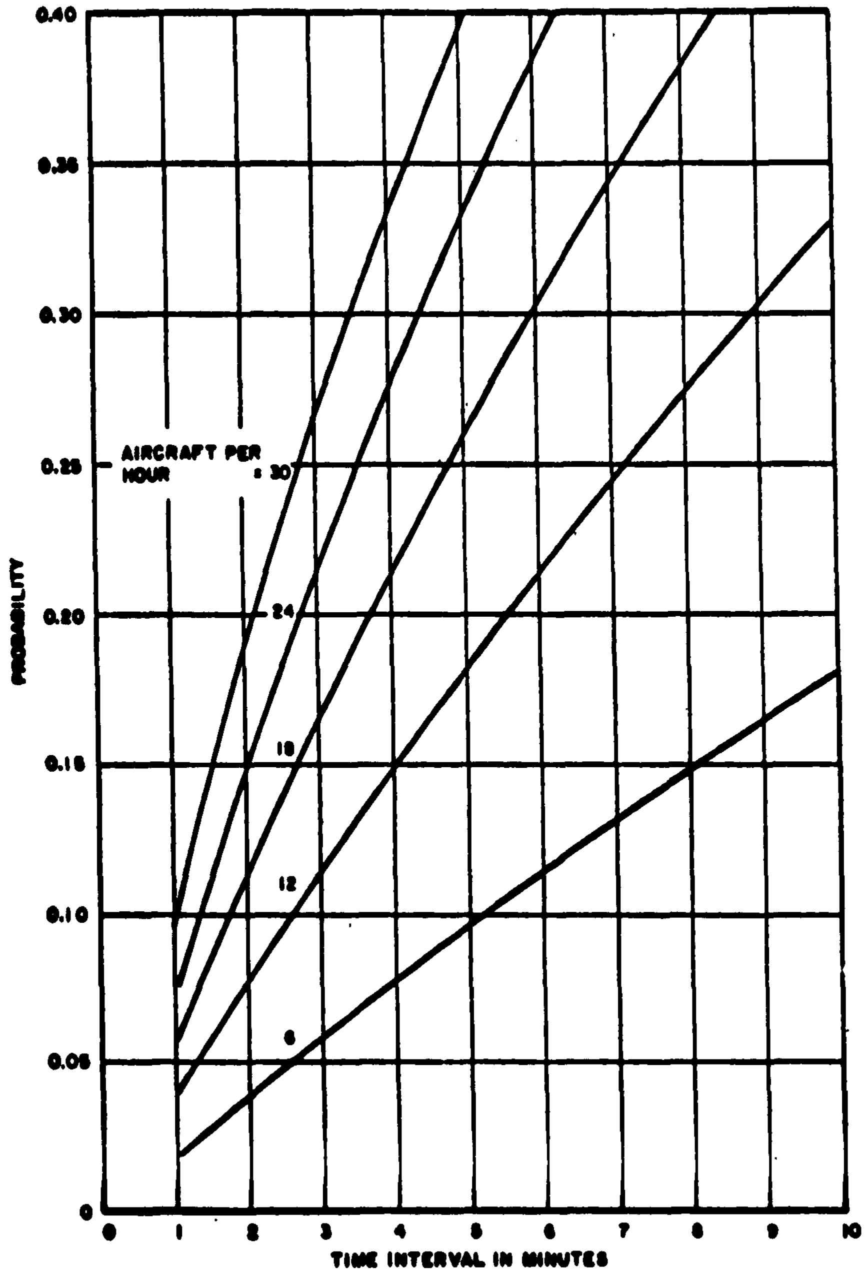

FIGURE A-2. PROBABILITY OF CONFLICT WITH 5 CODES

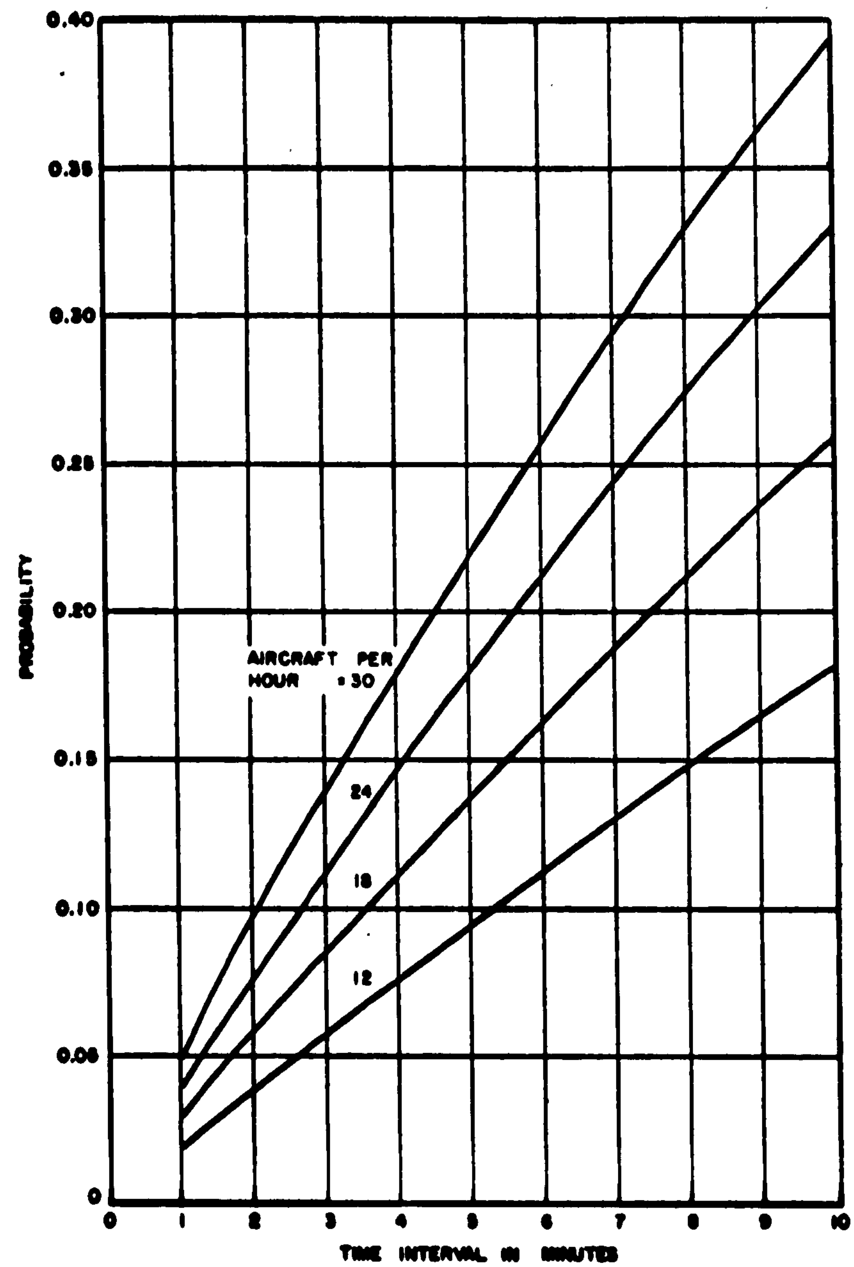

FIGURE A-3. PROBABILITY OF CONFLICT WITH 10 CODES

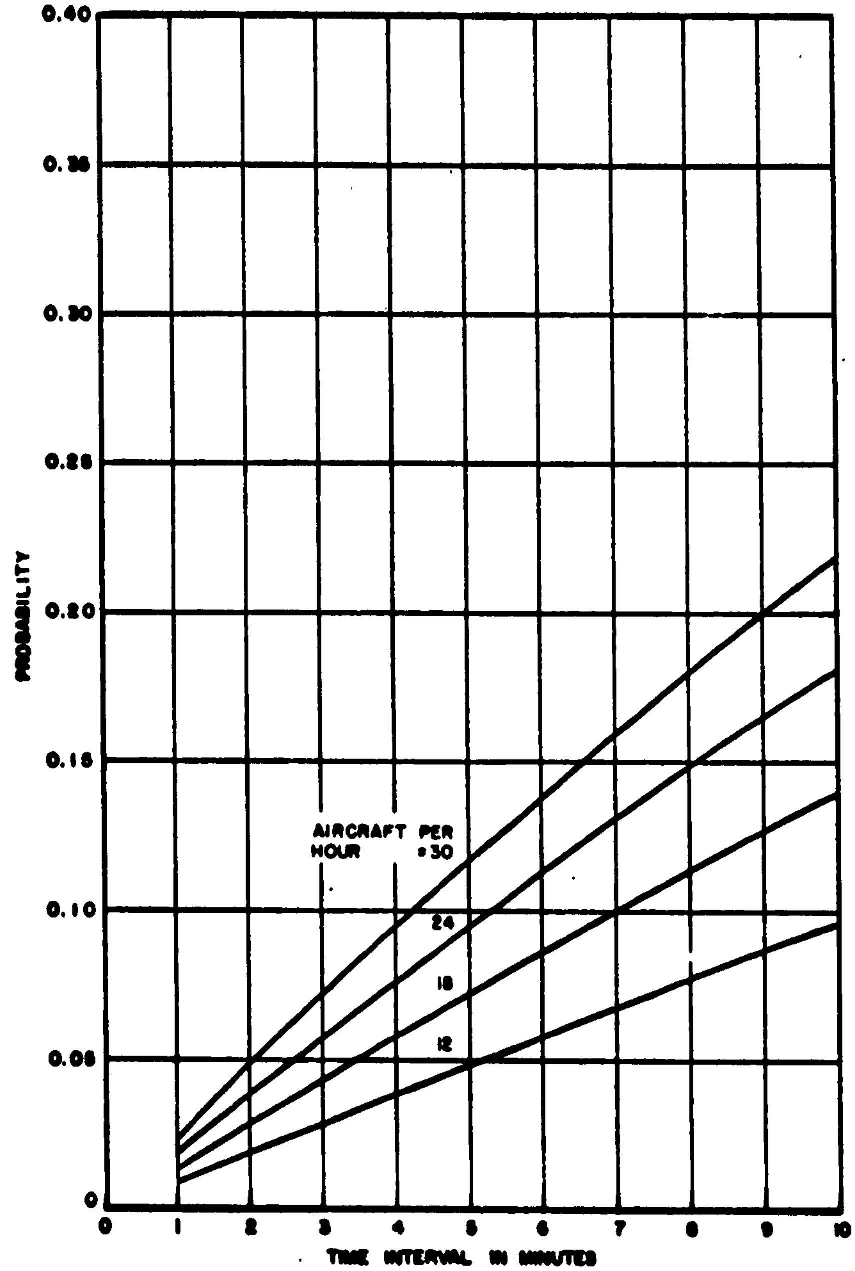

FIGURE A-4. PROBABILITY OF CONFLICT WITH 20 CODES

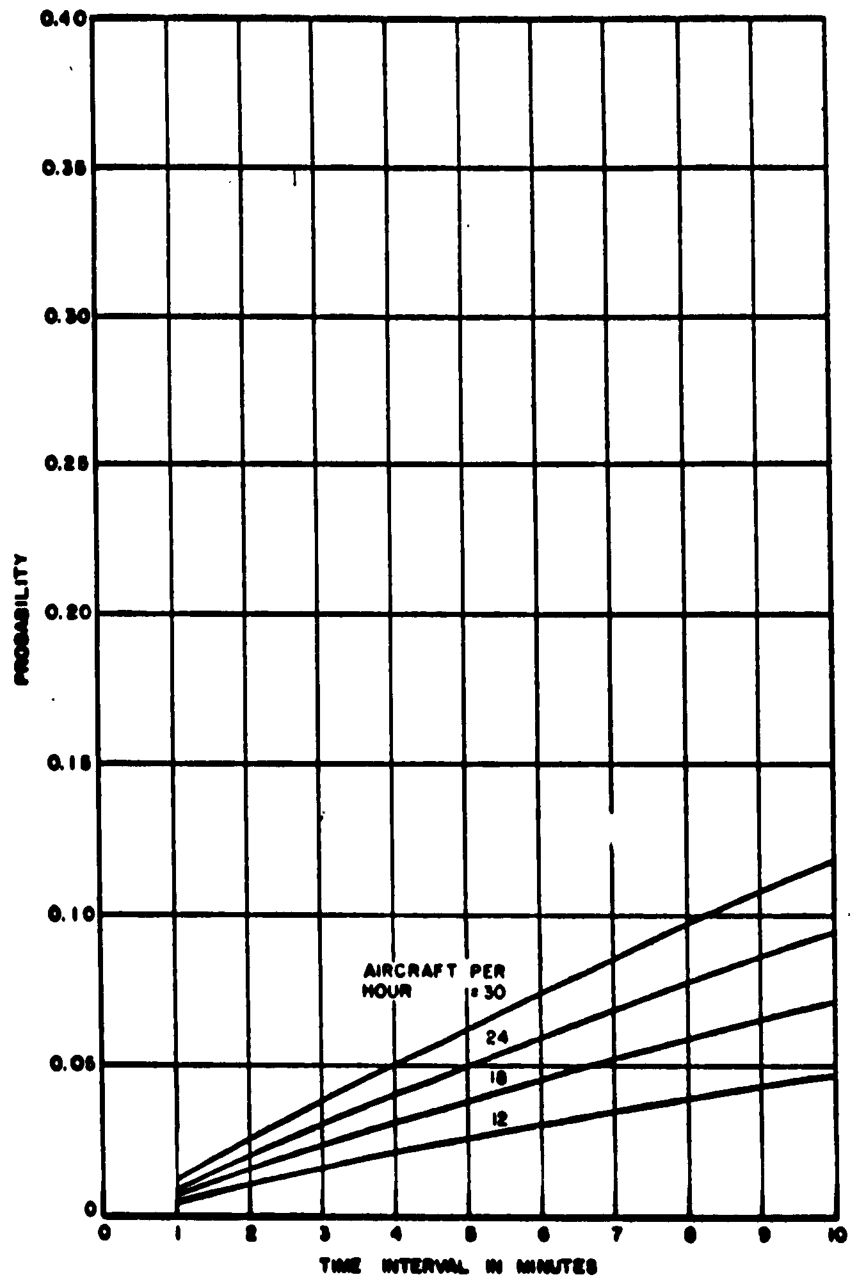

FIGURE A-5. PROBABILITY OF CONFLICT WITH 40 CODES

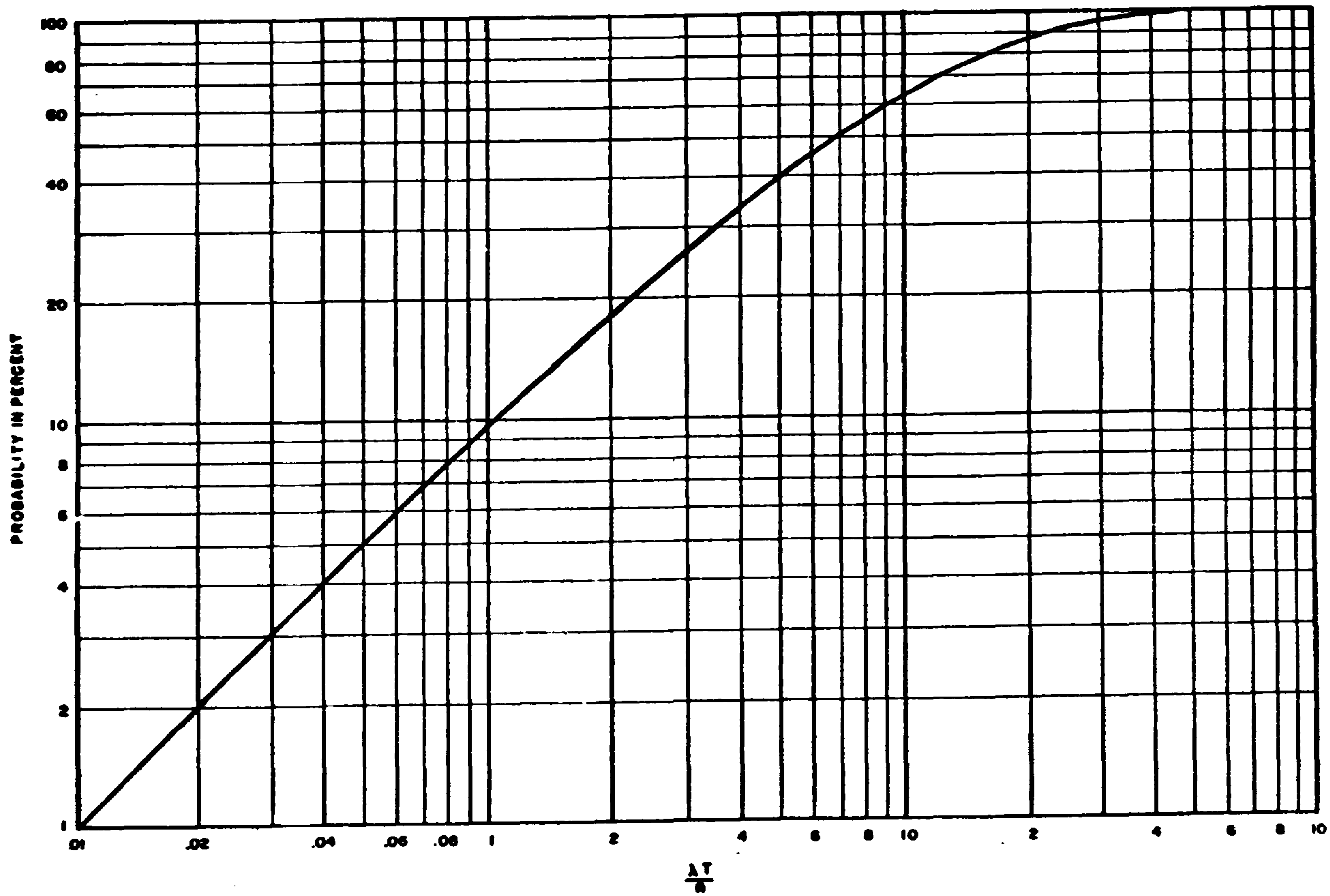

FIGURE A-6. PROBABILITY OF CONFLICT AS A FUNCTION OF AIRCRAFT DENSITY, TIME, AND NUMBER OF CODES

APPENDIX B

EFFECT OF CODE GARBLING ON A CODE-ASSIGNMENT PLAN

One of the factors to be considered in the development of a code-assignment plan is minimizing the probability of code garbling. Code garbling can occur in two principal ways: (1) garbling caused by fruit (nonsynchronous replies) from other transponders, and (2) garbling caused by another transponder at certain ranges within about 3.3 miles of the transponder of interest. The first type of garbling is non-synchronous and can be reduced significantly by use of a defruiter. The second type is synchronous and cannot be eliminated by a defruiter.

This investigation will be primarily concerned with minimizing the second type of garbling by judicious choice of codes. Codes that produce a large number of garbles can be used in widely separated areas to improve performance.

Code garbling has two effects. First, the code content of one or both of the interfering codes can be altered when a pulse from either pulse train coincides with an empty pulse position in the other train. Second, the pulses from the two trains can combine to appear as a fictitious target. This occurs whenever any two pulses, one from each train, are separated by 20.3 μsec plus or minus the decoder acceptance tolerance (normally ±0.45 μsec). The first case is called garbling and the second case false brackets.

False bracket generation can be shown to be a simple function of the number of information pulses present in each train. The number of positions where false brackets can be

generated, IF one pulse train is displaced within ±40.6 μsec with respect to the other train, is

$$N_b = 2(N_1 + 1)(N_2 + 1), \qquad \text{(B-1)}$$

where N_b is the number of false bracket positions and N_1 and N_2 are the number of information pulses present in each train. Figure B-1 shows a plot of equation B-1 for the various combinations of N_1 and N_2.

A simple function does not exist for the number of garbles because it is a function of the number and time position of the pulses. The number of garbles was counted manually. A chart was drawn up showing the 64 Mode 3/A codes. A movable plastic slide was fabricated and each code, in turn, was drawn on the slide with grease pencil. The slide was moved through the possible garble positions, and the number of garbles were recorded for each code-pair configuration--4096 combinations were investigated. Although the number of information pulses remained constant, the number of garbles varied. Generally, the variation in the number of garbles was only two or three; an average number of garbles, as a function of number of information pulses, seems to be useful information. Table B-I shows the result of the averaging process.

TABLE B-I

AVERAGE NUMBER OF GARBLE SITUATIONS

Number of Pulses in Interfering Code	Number of Pulses in Garbled Code 0	1	2	3	4	5	6
0	12	10	8	6	4	2	0
1	13	11.611	9.933	7.966	5.677	3	0
2	13	12.200	11.022	9.360	7.062	4	0
3	13	12.391	11.556	10.302	8.250	5	0
4	13	12.533	11.857	10.846	9.151	6	0
5	13	12.611	12.044	11.250	9.855	7	0
6	13	12.666	12.200	11.5	10.333	8	0

The same information, shown in Figure B-2, indicates that codes with most of the pulse positions filled are less susceptible to garbling. In general, however, the controller will be interested in the code content of both codes. Hence, Figure B-3 presents the average total number of garbles that can occur when an aircraft with N_1 pulses per reply is close to an aircraft with N_2 pulses per reply.

A factor that was not included in the garbling analysis is the position of the information pulses. It can be shown that, if several codes have the same number of information pulses, those codes with the first and last information pulses occupied will be less susceptible to garbling. For example, with three information pulses present, Codes 07, 16, 34, and 70 are least susceptible to garbling.

It can be concluded that situations demanding a minimum number of false targets should use codes with a minimum number of information pulses. Codes with many information pulses should be used when minimum garbling is required.

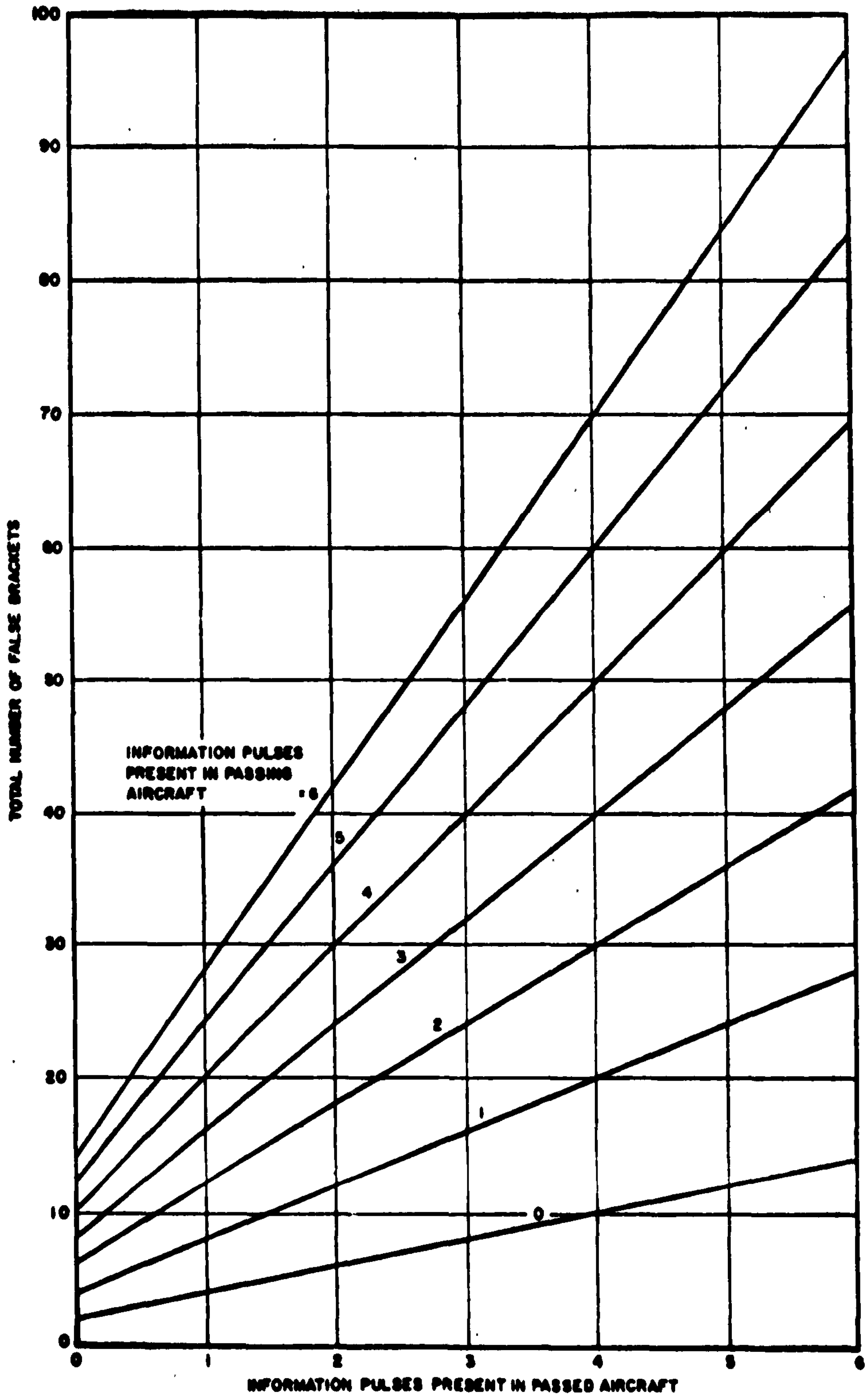

FIGURE B-1. FALSE BRACKET GENERATION AS A FUNCTION OF THE NUMBER OF INFORMATION PULSES PRESENT IN TWO AIRCRAFT EXERCISING A PASSING MANEUVER

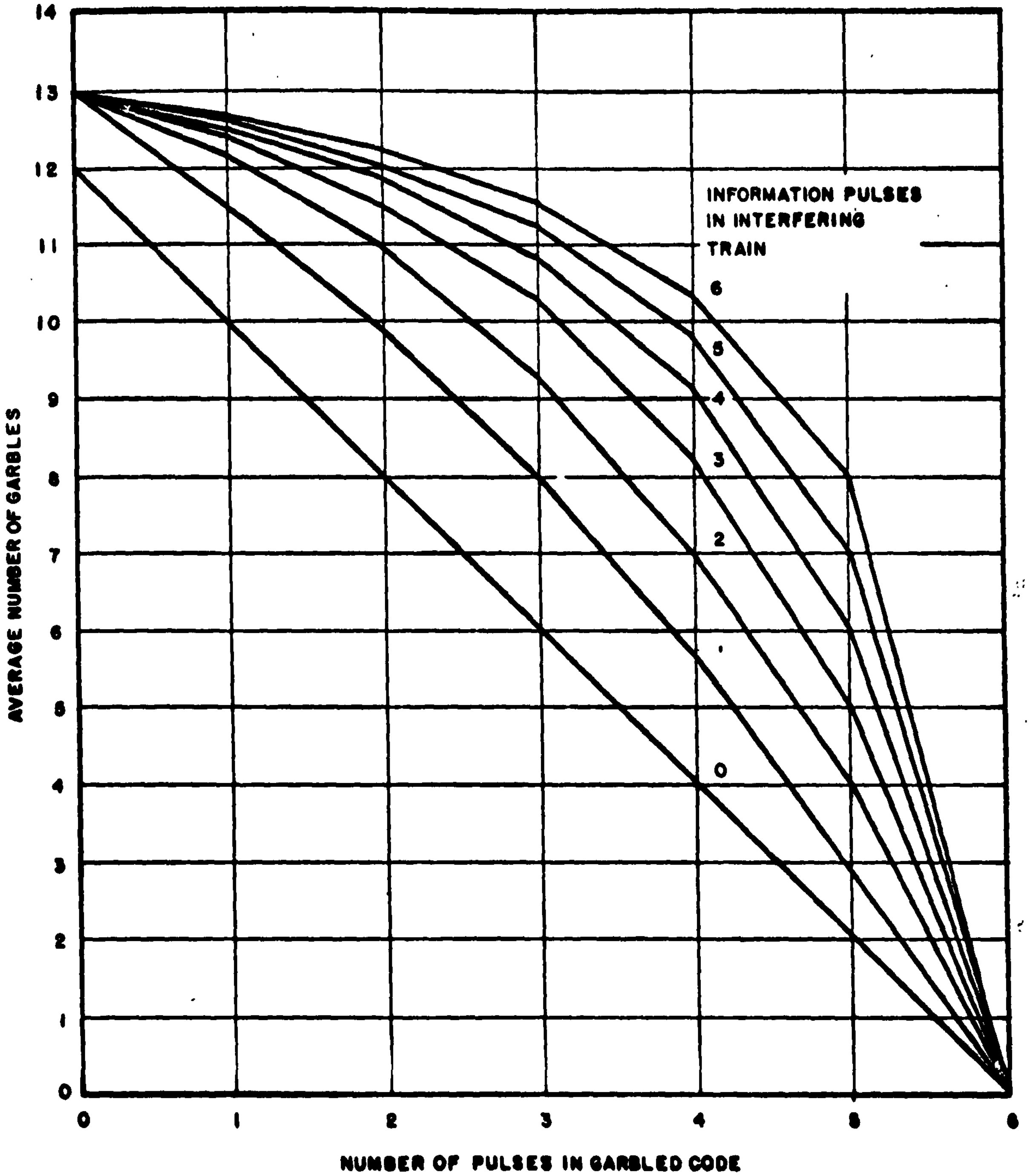

FIGURE B-2. CODE GARBLING AS A FUNCTION OF THE NUMBER OF INFORMATION PULSES PRESENT IN TWO AIRCRAFT EXERCISING A PASSING MANEUVER

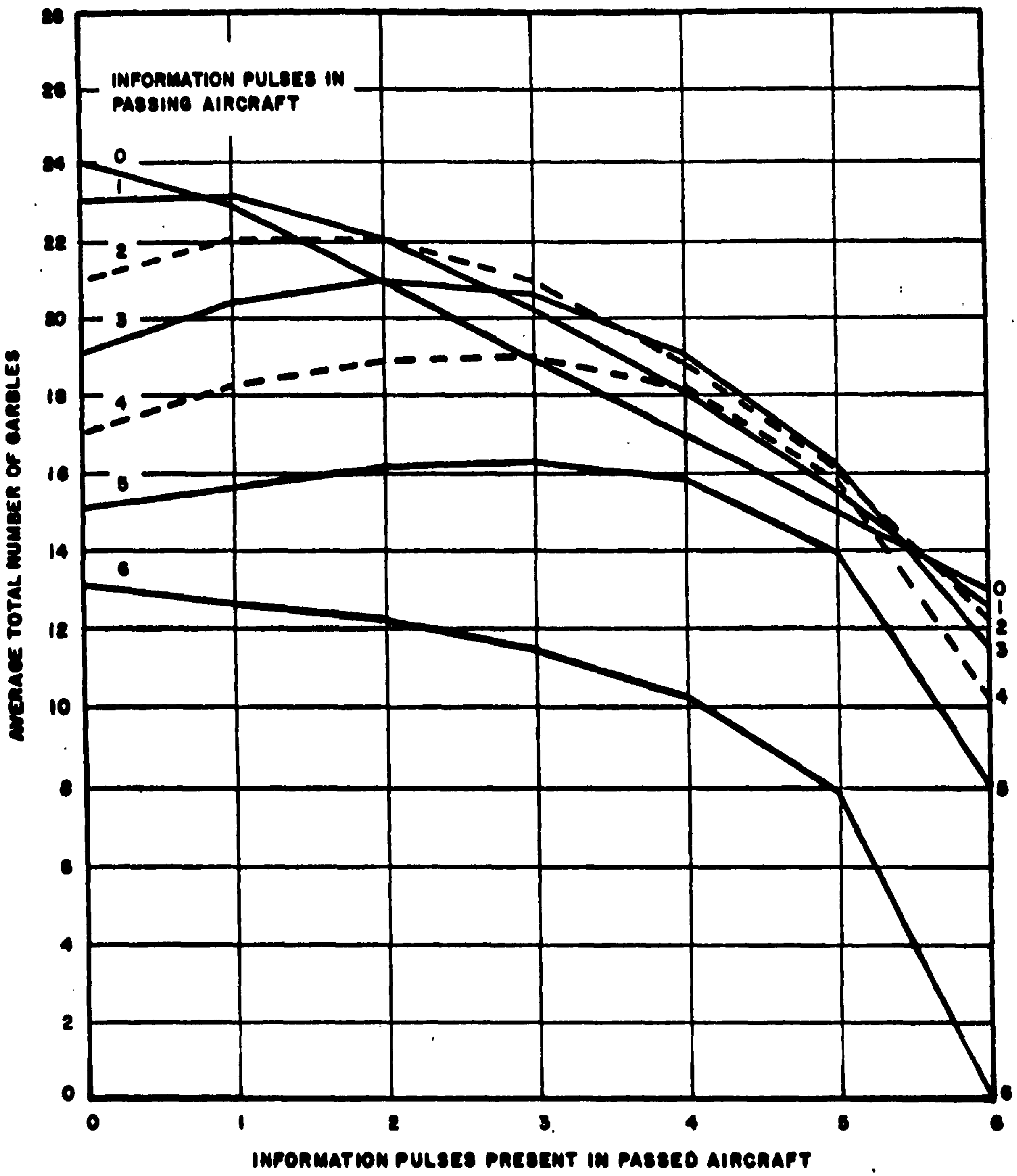

FIGURE B-3. TOTAL CODE GARBLING (TO BOTH CODES) AS A FUNCTION OF THE NUMBER OF INFORMATION PULSES PRESENT IN TWO AIRCRAFT EXERCISING A PASSING MANEUVER

APPENDIX C
ANALYSIS OF AN/FST-2

I. TARGET DETECTION, RELEASE, AND CENTER MARKING

A sequential observer is a data processor that counts $+\alpha$ for each success and $-\beta$ for each failure and decides that a particular event has occurred when the total count reaches or exceeds γ. The count is not permitted to become negative. The decision is irrevocable when the count reaches or exceeds γ. Each possible count from 0 to γ is defined as a unique state. Since the mechanism is completely characterized by a number of discrete states--in which the conditional probability of a transition from any state m to another state n is independent of the history of the system before reaching state m--the random process is a Markov process. If p is the probability of success, q is the probability of a failure, and P_j^i is the probability of being in the j^{th} state on the i^{th} trial, the following set of iterative state equations can be written for the general case of a sequential observer where $\alpha \geq \beta$ and $\gamma > 0$.

$$P_o^{i+1} = qP_o^i + qP_1^i + \cdots + qP_\beta^i$$

$$\vdots$$

$$P_j^{i+1} = pP_{j-\alpha}^i + qP_{j+\beta}^i \qquad \left| \begin{array}{l} \text{when } j < \alpha,\ P_{j-\alpha}^i = 0 \\ \text{when } j \geq \gamma - \beta,\ P_{j+\beta}^i = 0 \end{array} \right.$$

$$\vdots$$

$$P_\gamma^{i+1} = pP_{\gamma-\alpha}^i + pP_{\gamma-\alpha+1}^i + \cdots + P_\gamma^i$$

53

civil aircraft can reply only to Mode 3/A interrogations, it is necessary to equate p to zero and q to 1 whenever an iteration corresponding to a Mode 2 interrogation is performed. The sequential observer operates in the same manner for target release, with the exception that a failure counts $+\alpha$ and a success counts $-\beta$. Hence, the release matrix is identical to the detection matrix except that p and q have been redefined. Interlace is treated in the same manner. The following cases were considered:

I. Detection of a military aircraft.
II. Detection of a civil aircraft.
III. Release of a military aircraft.
IV. Release of a civil aircraft.

Four initial conditions for starting the interlace cycle in Case II are evaluated (2-3-3-3, 3-3-3-2, 3-3-2-3, and 3-2-3-3) and the probability of detection is determined by averaging the probabilities of all four conditions. Detection at the end of the 3-3-3-2 interlace cycle is impossible because detection cannot occur on a Mode 2 interrogation. Thus, the release of a target on that cycle is not considered. Only the remaining three ways are possible, and the average of the three resulting conditions is determined.

It is necessary to pair appropriate release and detection probabilities for the center marking analysis. For example, if detection occurred on the last Mode 3 interrogation in a group, the release cycle would start with 2-3-3-3. A portion of a sample data sheet for determining probability of center marking is shown in Table C-I.

The first column indicates detection on hit 10, 11, 12, 13...50. Column 2 is always equal to twice the number of hits at center mark minus Column 1. Column 3 is equal to 50 minus Column 1. Column 4 is equal to Column 2 minus Column 1. When Column 4 is equal to or less than Column 3, the

TABLE C-I

PROBABILITY OF CENTER MARK AT HIT 33.5
(ROUND RELIABILITY 0.7)

Detection Hit No.	Release Hit No.	Hits in Beamwidth After Detection	Interrogation to Release After Detection	Interlace Cycle After Detection	Probability of Detection P_d	Probability of Release P_r	Joint Probability P_dP_r
10	57	40	47	3	0	-	0
				1	.0576	.0030	.0002
				2	.0576	.0021	.0001
11	56	39	45	2	.0576	.0051	.0003
				3	.0576	.0036	.0002
				1	.1384	.0044	.0006
12	55	38	43	1	.1384	.0150	.0021
				2	.0173	.0096	.0002
				3	.0173	.0213	.0004
13	54	37	41	1	.1263	.0272	.0034
				2	.0900	.0429	.0039
				3	.0052	.0321	.0002
14	53	36	39	3	.0052	.0472	.0002
				1	.1650	.0377	.0062
				2	.1287	.0531	.0068
⋮	⋮	⋮	⋮	⋮	⋮	⋮	⋮

$$\Sigma = .1123$$

$$\frac{\Sigma}{4} = .0281$$

probability of release is equal to the probability of having attained state $\gamma \geq 13$ on that trial. When Column 4 is greater than Column 3, the end of the beam has been reached before the target is released; the difference Δ between Column 3 and Column 4 indicates the number of post-release trials and hence specifies the state or states the counter can be in at the end of the beam and the corresponding probability. The states are equal to $14 - 2\Delta$ and $13 - 2\Delta$. Since negative states do not exist, when $\Delta = 7$, only the zero state is possible. Column 5 is an arbitrary designation for the interlace cycle after detection that was used consistently throughout. Actually, a fourth cycle exists with a probability of zero since detection cannot take place on a Mode 2 interrogation. As shown in the table, probability of detection P_d is multiplied by the probability of release P_r to determine the joint probability. These joint probabilities are summed, and the average is determined by dividing by four.

II. MODE 3 CODE ANALYSIS

A. PULSE X MISLABELING

Methods of estimating the extent of Pulse X mislabeling are developed for three conditions:

1. A single Pulse X return is required for mislabeling.
2. Two returns in a row are required for mislabeling.
3. A defruited Pulse X return is required for mislabeling.

The analysis is restricted to false labeling of a Mode 3/A reply by Mode 3/A fruit. It is assumed that Mode 3/A codes are average 5-pulse codes and that the leading edge of the interfering pulse is detectable within a range of 0.9 μsec relative to the code train.

1. SINGLE LABEL IN m HITS

Before proceeding with the analysis, it is necessary to define the Poisson probability distribution. The probability of exactly j events occurring in a specific interval when the average or expected number during this interval is λ, is

$$p(j,\lambda) = \frac{\lambda^j e^{-\lambda}}{j!} \qquad \text{(C-1)}$$

provided that the number of events is large and the interval of test is small--that is, if λ is of moderate magnitude, as it is for all cases considered. Furthermore, the probability of exactly zero events is

$$1 - \sum_{j=1}^{\infty} \frac{\lambda^j e^{-\lambda}}{j!} = e^{-\lambda} \qquad \text{(C-2)}$$

as also given by the Poisson distribution for $j = 0$.

There are eight possible positions where a fruit reply group may result in a false label of the synchronous Mode 3/A code. Two of the eight positions involve a bracket pulse and will always mislabel. Thus, the probability that the reply will not be mislabeled as a result of brackets is the probability that no starts occur in these two positions--that is,

$$p_b = (e^{-\lambda})^2, \qquad \text{(C-3)}$$

where λ is the average or expected number of fruit reply groups that start in any randomly selected 0.9-μsec interval.

When the interfering pulse train starts in a position where an information pulse position coincides with the center pulse position, the probability that the target is not mislabeled is equal to the sum of (1) the probability that a group does not start at that position, (2) the probability that if it does start, the corresponding pulse position that aligns with the label position is absent, (3) the probability that if two groups start, the alignment pulse is absent on both groups, etc. This situation is descriptive of six positions, so that the probability of not mislabeling as a result of these positions is

$$
\begin{aligned}
p_1 &= \left[e^{-\lambda} + \lambda e^{-\lambda}(p_o) + \frac{\lambda^2}{2!} e^{-\lambda}(p_o)^2 + \dots\right]^6 \\
&= e^{-6\lambda(1-p_o)}
\end{aligned}
\tag{C-4}
$$

where p_o is the probability of absence of the internal code pulses at each position. Thus,

$$p_o = \frac{n - k}{n - 2}, \tag{C-5}$$

where n is the maximum number of pulse positions (eight for Mode 3/A) and k is the number of pulses (including the bracket pulses) present in the group. For example, for an average Mode 3/A code, $k = 5$ and $p_o = 1/2$.

Combining equations C-3 and C-4 as a joint probability function yields the overall probability of not mislabeling a reply as a Pulse X reply:

$$p_s = e^{-\lambda(8-6p_o)} \tag{C-6}$$

or more generally

$$p_s = e^{-\left[n-(n-2)p_o\right]\lambda} \qquad (C-7)$$

which reduces to

$$p_s = e^{-k\lambda} \qquad (C-8)$$

Since $\lambda = fT$, where f is the fruit rate per second and T is the range of acceptance (0.9 µsec),

$$p_s = e^{-fTk}. \qquad (C-9)$$

If there are m hits after detection, the probability of no false labels within the beamwidth is

$$p = p_s^m = e^{-fTkm} \qquad (C-10)$$

and hence the probability of a false Pulse X label for the target is

$$Q = 1 - e^{fTkm}$$

2. PULSE X INTEGRATION

Pulse X integration, or requiring two Pulse X returns in a row, corresponds to a sequential observer with $\alpha = 1$, $\beta = -1$, $\gamma = 2$. The matrix transform is

$$A = \begin{bmatrix} q & q & 0 \\ p & 0 & 0 \\ 0 & p & 1 \end{bmatrix}$$

As in the detection analysis, p is equal to zero on an iteration corresponding to a Mode 2 interrogation. The probability that the parity requirement will be satisfied when the center pulse is occupied by a fruit pulse is about 0.5. Therefore, a value of p equal to $e^{-fTk}/2$ is used for numerical evaluation.

3. DEFRUITING

In a single defruiter, n_t pulses of incoming fruit of duration T_u are delayed by the pulse-recurrence period and compared in a coincidence-gate circuit for synchronism. The delayed pulses are stretched to duration T_d before comparison is made. All synchronous signals generate outputs from the coincidence gate whereas nonsynchronous signals are rejected. In a high-density environment, however, there is a significant probability that coincidence may occur between random, non-synchronous fruit pulses. The number of random coincident pulses passed by the defruiter will be determined and its effect on Pulse X mislabeling evaluated.

Since these coincidence pulses have a finite probability of overlap with one another, the number of discrete pulses n_c can be determined by considering the number of discrete pulses on the delayed and undelayed channels. These are obtained by modifying n_t by the probability that exactly zero pulses occur during a pulse duration. For the undelayed and delayed lines respectively, they are

$$n_u = n_t e^{-n_t T_u} \qquad \text{(C-11)}$$

and

$$n_d = n_t e^{-n_t T_d}. \qquad \text{(C-12)}$$

The number of discrete coincidence gates generated can now be determined by considering the two ways in which the n_c and n_u pulses may combine. This is given by the probability that one or more pulses exist on the delayed line times n_u, plus the converse--one or more pulses exist on the undelayed line times n_d; that is

$$n_c = n_u \left[1 - e^{-n_t(T_d - d)}\right] + n_d \left[1 - e^{-n_t(T_u - d)}\right], \quad \text{(C-13)}$$

where d is the minimum allowable pulse overlap dictated by finite bandwidth requirements. Substituting equations C-11 and C-12 into C-13 yields

$$n_c = n_t \left\{ e^{-n_t T_u} \left[1 - e^{n_t(T_d - d)}\right] + e^{-n_t T_d} \left[1 - e^{-n_t(T_u - d)}\right] \right\} \quad \text{(C-14)}$$

The probability of a false Pulse X out of the defruiter is the sum of (1) the probability of joint occurrence of an n_t pulse on the delayed and undelayed defruiter lines coinciding with the leading edge of the center pulse position of the valid reply, and (2) the probability that, if this does not occur, the leading edge n_c will start within a pulse width T_u. That is,

$$p_n = \left[1 - e^{-n_t(T_u - d)}\right]\left[1 - e^{-n_t(T_d - d)}\right] + \left\{1 - \left[1 - e^{-n_t(t_u - d)}\right]\left[1 - e^{-n_t(T_d - d)}\right]\right\}\left(1 - e^{-n_c T_u}\right), \quad \text{(C-15)}$$

or the probability of success (probability of not mislabeling) is

$$p_a = e^{-n_c T_u} \left\{1 - \left[1 - e^{-n_t(T_u - d)}\right]\left[1 - e^{-n_t(T_d - d)}\right]\right\} \quad \text{(C-16)}$$

which, it will be noted, is the joint probability that neither event occurs.

If there are m hits in the beamwidth in the mode or modes on which the aircraft is replying, the probability of no false label in a beamwidth is

$$P = (1 - p_a)^m \qquad \text{(C-17)}$$

and the probability of at least one false label is

$$Q = 1 - (1 - p_a)^m.$$

The values of T_u = 0.45 μsec, T_d = 1.5 μsec, and d = 0.2 μsec were used in numerical evaluation.

4. DEFRUITING PLUS PARITY

With parity checking, single hit probability of mislabeling is again decreased by one-half.

5. EFFECT OF ROUND RELIABILITY

The single-hit probability of mislabeling in each case is based on receiving a valid reply on each interrogation. In a practical situation, replies are not received on each interrogation. The round reliability expresses the probability that a reply is received. If p_s is the single-hit probability of mislabeling and p_r is the round reliability, the reduced single-hit probability of mislabeling p_s' is

$$p_s' = p_s p_r.$$

A round reliability of 0.9 was assumed in all calculations.

B. MODE 2 MISLABELING

1. EXISTING AN/FST-2

The Poisson probability distribution of exactly zero events is $e^{-\lambda}$ where λ is the average or expected number of events. If N is the total number of range quanta per scan, C is the fruit rate per scan, and 60 percent of this fruit has proper parity, the average rate of false Mode 2 replies per quantum is

$$\lambda = \frac{0.6C}{N},$$

then

$$p_s = e^{\frac{-0.6C}{N}} \cong 1 - 0.6\frac{C}{N} \qquad \text{(C-18)}$$

If there are m Mode 2 post-detection interrogations, the probability of not mislabeling is

$$p = (1 - 0.6\frac{C}{N})^m .$$

2. MODE 2 INTEGRATION

Mode 2 integration, as postulated, requires two returns with proper parity before the label is changed. The replies do not have to be identical. A sequential observer with $\alpha = 1$, $\beta = 1$, and $\gamma = 2$ is equivalent to two-in-a-row integration with

$$p = e^{\frac{-0.6C}{N}}.$$

3. DEFRUITING

In order for a Mode 2 label to be passed by the defruiter, there must be coincidence at both bracket-pulse

positions. The single-hit probability of a mislabel is given by

$$p = p_a^{\,2},$$

where p_a is given by equation C-16. The probability of not mislabeling during a beamwidth with m Mode 2 interrogations is

$$P = (1 - p_a^{\,2})^m.$$

At the fruit rates under consideration, the numerical value of the probability of mislabeling with defruiting and/or parity is negligible.

C. CODE GARBLING

The Mode 3/A code structure contains six information bits, as shown in Figure C-1. There are 13 positions where fruit replies can be initiated and result in a garble of the desired reply. It is assumed that the interference is from Mode 3/A replies only. This assumption is a good approximation in a typical environment since a high percentage of the fruit consists of Mode 3/A replies.

An examination of the 13 positions shown in Figure C-1 reveals that, for any given position, (1) one bracket pulse of the interference group can contribute to a garble, and (2) one or more internal pulses can contribute to a garble. If p_r is the probability that a pulse is present in a given position in the 6-bit code structure, and p_f is the probability of the presence of a pulse in a particular position in the interference group, the probability of success p_1 for the desired code when only a bracket pulse of the

interference group can cause a garble (for example, positions 1 and 13) is

$$p_1 = p_r + (1 - p_r)e^{-\lambda}, \tag{C-19}$$

where λ is the average number of starts at a given position and $e^{-\lambda}$ is the Poisson probability of exactly zero such starts. The subscript on p_s (p_1 in this case) denotes position number. The equation reads that either the vulnerable pulse position of the desired code is occupied or, if it is vacant, that no interference groups can start. (Note that $p_f = 1$ for bracket-pulse interference.)

If a fruit group starts at a position where only one of its internal pulses can cause interference (for example, position 2) and if A is the event that the internal pulse in the desired group is present and B is the event that the interference pulse position is vacant, then the probability of success at that position is the union of A and B.

$$\begin{aligned} P(AUB) &= P(A) + P(B) - P(AB) \\ &= p_r + (1 - p_f) - p_r(1 - p_f). \end{aligned} \tag{C-20}$$

If two fruit groups start at the same position (still position 2, for example) and C is the event that the interfering pulse position in the second interference group is vacant, then the probability of success is

$$\begin{aligned} P\left[(AUBC)\ U\ (A'BC)\right] &= P(A) + P(BC) - P(ABC) \\ &= p_r + (1 - p_f)^2 - p_r(1 - p_f)^2. \end{aligned} \tag{C-21}$$

For three groups starting at that position and D as the event that the interfering pulse position is vacant, the probability of success is

$$P\left[(A \cup BCD) \cup (A'BCD)\right] = P(A) + P(BCD) - P(ABCD) \tag{C-22}$$

$$= p_r + (1 - p_f)^3 - p_r(1 - p_f)^3.$$

In general, for n fruit groups

$$P\left[(A \cup BCD\ldots) \cup (A'BCD\ldots)\right] = p_r + (1 - p_f)^n - p_r(1 - p_f)^n. \tag{C-23}$$

Given that one or more fruit groups have started at a given position, say n, and that associated with the potential internal-garbling position of the fruit group is a bracket pulse that can garble the valid code, the joint probability of success at that position is

$$p_n = p_r\left[p_r + (1 - p_f)^n - p_r(1 - p_f)^n\right]. \tag{C-24}$$

For a given start position with a single bracket-pulse interference and one eligible internal-pulse interference, the total probability of success at a given position is

$$\begin{aligned} p_{s\alpha} = e^{-\lambda} & \\ & + \lambda e^{-\lambda}\left\{p_r\left[p_r + (1 - p_f) - p_r(1 - p_f)\right]\right\} \\ & + \frac{\lambda^2 e^{-\lambda}}{2!}\left\{p_r\left[p_r + (1 - p_f)^2 - p_r(1 - p_f)^2\right]\right\} \\ & + \frac{\lambda^3 e^{-\lambda}}{3!}\left\{p_r\left[p_r + (1 - p_f)^3 - p_r(1 - p_f)^3\right]\right\} \\ & + \ldots \end{aligned} \tag{C-25}$$

where α denotes success at position α, a position where one bracket and one internal pulse are potential garbling sources. Each term in the series represents the disjoint probability of success given that n interference groups have started at that position.

Factoring and rearranging terms,

$$
\begin{aligned}
p_{s\alpha} = {} & e^{-\lambda} \\
& + p_r e^{-\lambda}\left[\lambda p_r + \lambda(1 - p_f) - \lambda p_r(1 - p_f)\right] \\
& + p_r e^{-\lambda}\left[\frac{\lambda^2}{2!} p_r + \frac{\lambda^2}{2!}(1 - p_f)^2 - \frac{\lambda^2 p_r}{2!}(1 - p_f)^2\right] \\
& + p_r e^{-\lambda}\left[\frac{\lambda^3}{3!} p_r + \frac{\lambda^3}{3!}(1 - p_f)^3 - \frac{\lambda^3 p_r}{3!}(1 - p_f)^3\right] \\
& + \cdots
\end{aligned}
\qquad \text{(C-26)}
$$

Summing terms vertically in equation C-26 and recognizing series expansions of $(e^{\lambda} - 1)$,

$$p_{s\alpha} = e^{-\lambda} + p_r^2 e^{-\lambda}(e^{\lambda} - 1) + p_r e^{-\lambda}\left[e^{\lambda(1-p_f)} - 1\right] - p_r^2 e^{-\lambda}\left[e^{\lambda(1-p_f)} - 1\right], \qquad \text{(C-27)}$$

which can be simplified to

$$p_{s\alpha} = p_r\left[p_r + e^{-\lambda p_f}(1 - p_r)\right] + (1 - p_r)e^{-\lambda}. \qquad \text{(C-28)}$$

Thus, the probability of success is equal to the joint probability of success (first term on right of equality sign) that

a pulse is present at the bracket position p_r and that no garbling occurs at the internal-pulse position,

$$\left[p_r + e^{-\lambda p_f}(1 - p_r)\right].$$

This latter term can be interpreted as meaning that either a pulse is present at the critical position in the desired code or, if it is absent, that no damaging interference groups are present. Note that the harmful groups are designated by modifying the λ exponent by p_f, the probability of occurrence of a pulse in the fruit group. The second term on the right of equation C-28 is the probability that the pulse position in the desired code corresponding to the bracket interference is vacant; in this event, for success, no interference groups can be initiated.

It follows that, for fruit alignment with one bracket pulse and m internal positions vulnerable to garbling, the probability of success at that position is

$$p_{s\alpha} = p_r\left[p_r + e^{-\lambda p_f}(1 - p_r)\right]^m + (1 - p_r)e^{-\lambda}. \qquad \text{(C-29)}$$

The total probability of success for the desired code is equal to the joint probability of success at all 13 start positions in Figure C-1. However, the individual probabilities are not stochastically independent, a condition that may be circumvented by considering the nondisjoint probabilities of garbling at each position. That is, if G_j is the event that a garble occurs at the j^{th} position.

$$P(G_1 \cup G_2 \cup G_3 \cup \ldots \cup G_{13}) =$$

$$= \sum_{\alpha=1}^{13}(1 - p_{s\alpha}) - \sum_{\substack{\alpha,\beta \\ \alpha\neq\beta}}(1 - p_{s\alpha})(1 - p_{s\beta}) + \sum_{\alpha,\beta,\gamma}(1 - p_{s\alpha})(1 - p_{s\beta})(1 - p_{s\gamma}) - \cdots \qquad \text{(C-30)}$$

$$= \sum_{\alpha=1}^{13} q_{s\alpha} - \sum_{\substack{\alpha,\beta \\ \alpha\neq\beta}} q_{s\alpha}q_{s\beta} + \cdots,$$

where $q_{s\alpha} = 1 - {}'p_{s\alpha}$. The complete evaluation of the equation involves 2^{13} computations. However, the numerical complexities may be greatly simplified by application of the multinomial theorem.

$$(q_{s1} + q_{s2} + \cdots + q_{s13})^n = \sum_{\lambda, u, v} \frac{n!}{\lambda! u! v! \cdots} q_{s1}^{\lambda} q_{s2}^{u} q_{s3}^{v} \cdots \tag{C-31}$$

For $n = 1$,

$$(q_{s1} + q_{s2} + \cdots + q_{s13}) \sum_{\alpha=1}^{13} q_{s\alpha}. \tag{C-32}$$

For $n = 2$,

$$(q_{s1} + q_{s2} + \cdots q_{s13})^2 = \sum_{\alpha=1}^{13} \left(q_{s\alpha}^2 \right) + 2 \sum_{\substack{\alpha, \beta \\ \alpha \neq \beta}} q_{s\alpha} q_{s\beta} \tag{C-33}$$

so that

$$\sum_{\substack{\alpha, \beta \\ \alpha \neq \beta}} q_{s\alpha} q_{s\beta} = \frac{\left(\sum_{\alpha=1}^{13} q_{s\alpha} \right)^2 - \sum_{\alpha=1}^{13} \left(q_{s\alpha}^2 \right)}{2}.$$

Similarly, from $n = 3$,

$$\sum_{\alpha, \beta, \gamma} q_{s\alpha} q_{s\beta} q_{s\gamma} = \frac{\left(\sum q_{s\alpha} \right)^3 + 2 \sum q_{s\alpha}^3 - 3 \sum q_{s\alpha}^2 \sum q_{s\alpha}}{6}. \tag{C-34}$$

Also, from n = 4,

$$\sum_{\substack{\alpha,\beta,\gamma,\delta \\ \alpha=\beta=\gamma=\delta}} q_{s\alpha}\, q_{s\beta}\, q_{s\gamma}\, q_{s\delta} = \frac{\left(\sum q_{s\alpha}\right)^4 - 3 \sum q_{s\alpha}{}^4 + 8 \sum q_{s\alpha}{}^3 \sum q_{s\alpha} - 6 \sum q_{s\alpha}{}^2 \left(\sum q_{s\alpha}\right)^2}{24}, \qquad \text{(C-35)}$$

and so on.

The result of applying the multinomial theorem has been to express the cross-product terms required for equation C-30 in terms of the sums of probabilities raised to integer powers, where the integer is a constant for each summation. Substitution of equations C-32 through C-35 into equation C-30 yields a solution for the first four terms of alternating converging series; higher-order terms may be added in a similar manner. Since the series is conditionally convergent, the error is no greater than the last term computed in the series.

Finally, the probability of success P_s is given as

$$P_s = 1 - Q. \qquad \text{(C-36)}$$

Note that $\lambda = f_r T$, where f_r is the number of fruit reply groups per second and T is the tolerance of a decoding position, or permissible jitter.

These results can be applied as a generalized solution to any code structure where the desired and interference code groups have a similar format to the PCM format of the beacon system.

Numerical evaluation was carried out for three unfilled pulse positions, which is the average number of unfilled positions.

When a defruiter is used in the system, the probability of success or probability of no garble is given by

$$P = p_a^{\,n},$$

where p_a is the probability of no garble in a single unfilled position from equation C-16 and n is the number of unfilled pulse positions.

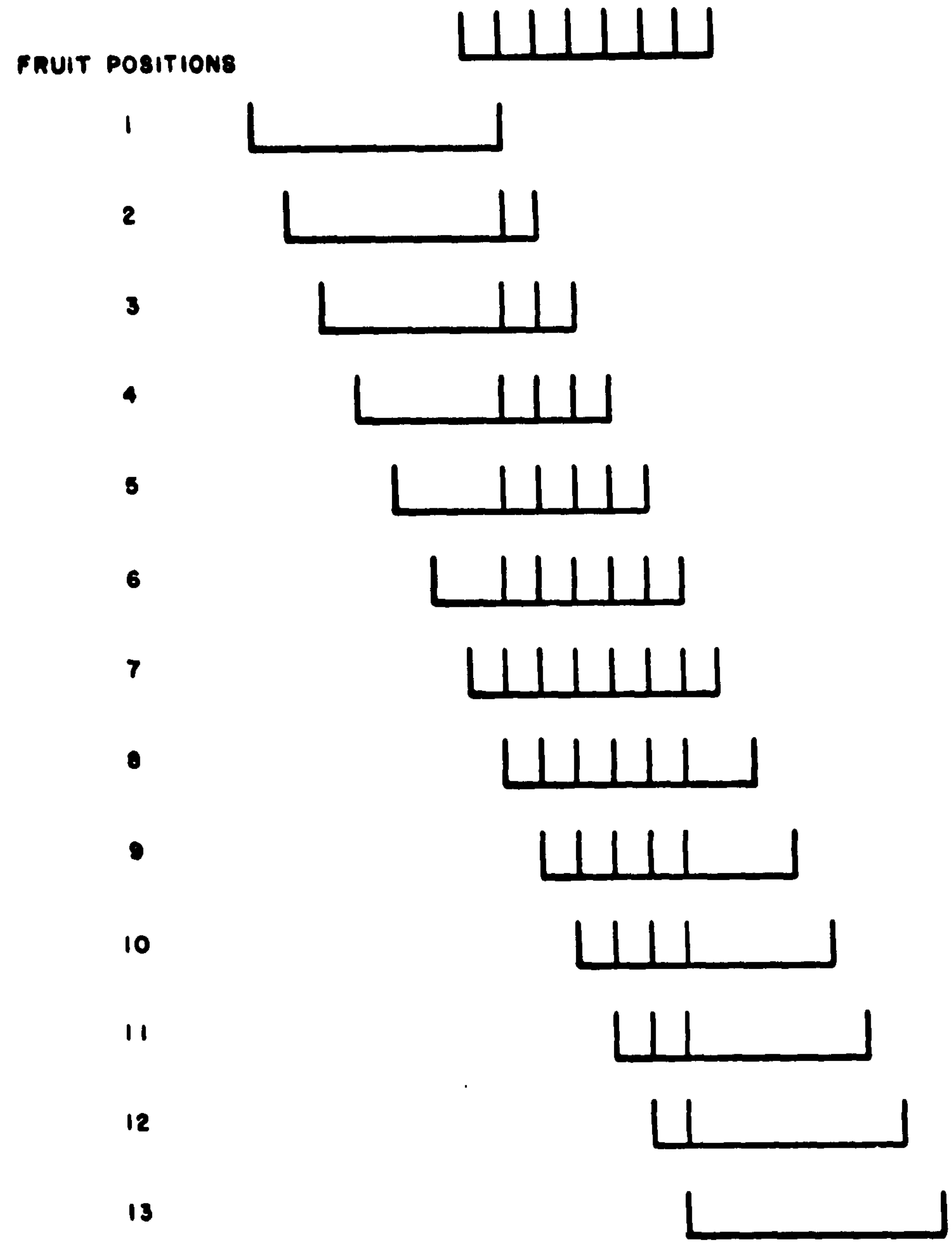

FIGURE C-1. POTENTIAL GARBLING POSITIONS FOR A REPLY CODE WITH 6 INFORMATION BITS

APPENDIX D
ANALYSIS OF SIF SCORE

The SIF score is also a Markov process, as defined in Appendix C, and can be handled by similar techniques. An eleventh-order matrix can be written by examining Figure 10. The rows and columns in the matrix are identified with the state designation from Figure 10. The small letters are used to denote the probability of an event in the flow chart. That is,

$$p = P(E)$$
$$z = P(Z)$$
$$g = P(G)$$
$$r = P(R)$$
$$n = P(N)$$

Also, since a garble is either the same as a garble used on the last scan or is different

$$g = r + n.$$

The resulting matrix is shown in Table D-1.

The probability of being in the j^{th} state on the i^{th} trial is

$$P_j^{i+1} = AP_k^i.$$

The probability of having an established code in the code being transmitted on the i^{th} trial is

$$P = P_0^i + P_2^i + P_4^i,$$

TABLE D-1

MATRIX REPRESENTATION OF SIF SCORE

$i+1 \diagdown i$	E_3	F_3	E_2	F_2	E_1	F_1	Z_0	V_1	W_1	V_2	W_2
E_3	p	0	p	0	0	0	0	0	0	p	0
F_3	0	r	0	r	0	0	0	0	0	0	r
E_2	(g+z)	0	0	0	p	0	0	0	0	0	0
F_2	0	(p+n+z)	0	0	0	r	0	0	0	0	0
E_1	0	0	(g+z)	0	0	0	0	0	0	0	0
F_1	0	0	0	(p+n+z)	0	0	0	0	0	0	0
Z_0	0	0	0	0	z	z	z	z	z	z	z
V_1	0	0	0	0	0	p	p	0	p	0	p
W_1	0	0	0	0	g	n	g	g	n	g	n
V_2	0	0	0	0	0	0	0	p	0	0	0
W_1	0	0	0	0	0	0	0	0	r	0	0

and the probability of having an established code in an erroneous code on the i^{th} trial is given by

$$P = P_1^i + P_3^i + P_5^i.$$

When a code has been filed in the flight plan, P_0^0 is equal to 1 and the remaining P_j^0 are equal to zero. When

no code has been filed, P_6^0 is equal to 1 and the remaining P_j^0 are equal to zero.

The analysis of the AN/FST-2 provided most of the necessary probabilities for numerical evaluation when a single AN/FST-2 provides data. Only the probabilities of a repeated garble and a nonrepeated garble were not computed. There are seven ways in which a garble can occur with an average three-pulse code. Three of these ways are more likely to occur since they require coincidence only at a single pulse position. A pessimistic assumption for the probability that a garble is the same as a previous garble was made--r equals g/4 and n equals 3g/4.

When more than one AN/FST-2 provide data on a track, the probabilities within the matrix must be redefined in terms of the probabilities of events in a single AN/FST-2. A correct code will be accepted and stored if a correct code is available from either AN/FST-2 when in states U1, U2, E_1, E_2, E_3, and ZO. A correct code will also be accepted if a correct code is available from either AN/FST-2 when in states W_1, W_2, F_1, F_2, and F_3, except when a repeated garble is available from either AN/FST-2. Since the probability of being in states W_1, W_2, F_1, F_2, and F_3 is low, it is assumed that a correct code will always be accepted if available. Similarly, it is assumed that a repeated garble will always be accepted, if available, except when a correct code is available; a nonrepeated garble will be used, if available, except when either a correct code or a repeated garble is available. No code data are used only when no code data are available from either AN/FST-2. These assumptions are expressed in the following equations, where the subscript denotes the number of AN/FST-2's supplying data.

$$p_2 = P\{E \cup E\} = 2p_1 - p_1^2$$

$$z_2 = P\{Z\ Z\} = z_1^2$$

$$r_2 = P\{R \cup R/E'\} = 2r_1(1 - p_1) - r_1^2$$

$$n_2 = P\{N \cup N/E'R'\} = 2n_1 z_1 + n_1^2$$